Timing and development of the Heise volcanic field, Snake River Plain, Idaho, western USA

Lisa A. Morgan†
U.S. Geological Survey, Federal Center, Box 25046, MS 966, Denver, Colorado 80225, USA

William C. McIntosh‡
New Mexico Bureau of Mines and Mineral Resources, 801 Leroy Place, Socorro, New Mexico 87801, USA

ABSTRACT

The Snake River Plain (SRP) developed over the last 16 Ma as a bimodal volcanic province in response to the southwest movement of the North American plate over a fixed melting anomaly. Volcanism along the SRP is dominated by eruptions of explosive high-silica rhyolites and represents some of the largest eruptions known. Basaltic eruptions represent the final stages of volcanism, forming a thin cap above voluminous rhyolitic deposits. Volcanism progressed, generally from west to east, along the plain episodically in successive volcanic fields comprised of nested caldera complexes with major caldera-forming eruptions within a particular field separated by ca. 0.5–1 Ma, similar to, and in continuation with, the present-day Yellowstone Plateau volcanic field. Passage of the North American plate over the melting anomaly at a particular point in time and space was accompanied by uplift, regional tectonism, massive explosive eruptions, and caldera subsidence, and followed by basaltic volcanism and general subsidence.

The Heise volcanic field in the eastern SRP, Idaho, represents an adjacent and slightly older field immediately to the southwest of the Yellowstone Plateau volcanic field. Five large-volume (>0.5 km^3) rhyolitic ignimbrites constitute a time-stratigraphic framework of late Miocene to early Pliocene volcanism for the study region. Field relations and high-precision $^{40}Ar/^{39}Ar$ age determinations establish that four of these regional ignimbrites were erupted from the Heise volcanic field and form the framework of the Heise Group. These are the Blacktail Creek Tuff (6.62 ± 0.03 Ma), Walcott Tuff (6.27 ± 0.04 Ma), Conant Creek Tuff (5.51 ± 0.13 Ma), and Kilgore Tuff (4.45 ± 0.05 Ma; all errors reported at ± 2σ). The fifth widespread ignimbrite in the region is the Arbon Valley Tuff Member of the Starlight Formation (10.21 ± 0.03 Ma), which erupted from a caldera source outside of the Heise volcanic field. These results establish the Conant Creek Tuff as a distinct and widespread ignimbrite in the Heise volcanic field, eliminating former confusion resulting from previous discordant K/Ar and fission-track dates.

New $^{40}Ar/^{39}Ar$ determinations, when combined with geochemical, lithologic, geophysical, and field data, define the volcanic and tectonic history of the Heise volcanic field and surrounding areas. Volcanic units erupted from the Heise volcanic field also provide temporal control for tectonic events associated with late Cenozoic extension in the Snake Range and with uplift of the Teton Range, Wyoming. In the Snake Range, movement of large (≥0.10 km^3) slide blocks of Mississippian limestone exposed 50 km to the east of the Heise field occurred between 6.3 and 5.5 Ma and may have been catastrophically triggered by the caldera eruption of the 5.51 ± 0.13-Ma Conant Creek Tuff. This slide block movement of ~300 vertical meters indicates that the Snake Range had significant relief by at least 5.5 Ma. In Jackson Hole, the distribution of outflow facies of the 4.45 ± 0.05-Ma Kilgore Tuff related to eruption from the Kilgore caldera in the Heise volcanic field on the eastern SRP indicates that the northern Teton Range was not a significant topographic feature at this time.

Keywords: eastern Snake River Plain, Heise volcanic field, uplift of northern Teton Range, Snake Range detachment, Arbon Valley Tuff, Heise Group.

INTRODUCTION

The Snake River Plain (SRP), one of the major physiographic, volcanic, and tectonic features of North America, is of critical importance in understanding the geologic evolution of the Great Basin and northern Basin and Range provinces. The SRP is dominated by large-volume (>0.5 km^3) explosive eruptives of high-silica rhyolites from a series of nested caldera complexes, referred to as volcanic fields. The volcanic fields show an age progression from 16 Ma in the McDermitt volcanic field in southeastern Oregon to 2.05–0.64 Ma in the present-day Yellowstone Plateau volcanic field (Christiansen and Blank, 1969; Morgan, 1972; Armstrong et al., 1975; Anders et al., 1989; Richards et al., 1989; Pierce and Morgan, 1992; Malde, 1991; Smith and Braile, 1994; Christiansen, 2001). The systematic age-progression of SRP volcanism is clearly related to southwesterly movement of the North American plate over a mantle heat anomaly, although currently there is considerable debate over the depth of this hot spot and whether it is related to whole-mantle convection or upper mantle processes (Humphreys et al., 2000; Christiansen, 2001; Christiansen et al., 2002). In this paper, we use the term "hot spot" in its most general sense, referring to a stationary mantle source regardless of depth of origin or convective process. Recent evidence has suggested that initiation of this hot spot or thermal plume produced a large-volume magmatic plume head that affected an area at least 500 km in diameter (Pierce and Morgan, 1992; Camp, 1995; Pierce et al., 2004).

Detailed studies of SRP volcanism are important because: (1) eruption of high-silica rhyolitic ignimbrites and associated ash-fall deposits from SRP volcanic fields represent some of the largest and most destructive eruptions in Earth history, with estimated volumes of individual eruptions exceeding 1000 km^3, significantly impacting climate and biota communities (local extinction

†E-mail: lmorgan@usgs.gov.
‡E-mail: mcintosh@nmt.edu.

GSA Bulletin; March/April 2005; v. 117; no. 3/4; p. 288–306; doi: 10.1130/B25519.1; 12 figures; 2 tables; Data Repository item 2005059.

events) (Thompson et al., 1982; Rampino, 1991); (2) SRP volcanic fields represent fossil Yellowstone systems and detailed studies allow better understanding of temporal and spatial evolution of these caldera systems so that potential volcanic hazards in the still-active Yellowstone system can be better understood; (3) SRP volcanic fields provide an exceptional opportunity to understand a 16-Ma, time- and spatially transgressive volcanic system while also examining eruptive processes from large, nested caldera complexes; (4) these massive eruptions are related to regional tectonic events and movement of major slide blocks; (5) in some cases, the timing and distribution of ignimbrites from the Heise volcanic field provide critical time lines regarding uplift of mountain ranges; and (6) the related plinian pyroclastic material formed widespread deposits that help provide a chronostratigraphic framework for the western United States and adjacent northeast Pacific Ocean basin and Gulf of Mexico (Izett, 1981; Sarna-Wojcicki et al., 1987; Perkins et al., 1998; Perkins and Nash, 2002).

Establishing comprehensive stratigraphic correlations within the Heise volcanic field has required careful field studies and high-precision geochronology of sparsely distributed individual volcanic units, which are limited to discontinuous exposures along the margins of the Snake River Plain in the foothills of the surrounding Basin and Range mountains (Fig. 1). In some places, this has resulted in multiple local names for exposures of the same lithostratigraphic unit. Over the last twenty years, however, great advances have been made in correlating ignimbrites of regional extent between separate ranges as well as across the SRP (McBroome et al., 1981; Morgan et al., 1984; Morgan, 1992; Kellogg et al., 1994). These correlations are based on lithologic characteristics, mineralogy and phenocryst content, stratigraphic position, geochemical and isotopic characteristics, paleomagnetic directions, and $^{40}Ar/^{39}Ar$, K/Ar, and fission-track age determinations. Applying the high-precision, single-crystal $^{40}Ar/^{39}Ar$ dating method further refines those correlations. Determining the correlation of the regionally extensive ignimbrites with rhyolites that have a more limited distribution is important in understanding their temporal and physical relationship. Furthermore, single-crystal $^{40}Ar/^{39}Ar$ age determinations permit an improved evaluation of the timing of major episodes of volcanism on the SRP in relation to the volcanic history of the Heise volcanic field. Finally, determining the ages of these volcanic events provides insight into the timing of regional tectonic events.

In this paper, $^{40}Ar/^{39}Ar$ dating methods are used to tightly bracket the timing of major volcanic events in the Heise volcanic field. Five precisely dated, large-volume ignimbrites constitute a time-stratigraphic framework for this complex rhyolitic volcanic field. Four of these ignimbrites, referred to as the Heise Group, were erupted from the Heise volcanic field. Two of these ignimbrites are formally named in this paper. The fifth regional ignimbrite erupted from a caldera source southeast and adjacent to the Heise volcanic field (Pierce and Morgan, 1992; Kellogg et al., 1994). The $^{40}Ar/^{39}Ar$ data, in conjunction with chemical, isotopic, and other physical characteristics, also allow accurate correlation between distal and proximal facies of regional units.

GEOLOGIC FRAMEWORK

The Heise volcanic field is the next youngest of several volcanic fields identified in the Snake River Plain-Yellowstone Plateau volcanic province (Pierce and Morgan, 1992; Fig. 1). The 700 km by 90 km northeast-trending province cuts across the northern Basin and Range Province and disrupts the continuity of the older Sevier-Laramide orogenic belt. This province is bounded on the southwest by the ca. 16–14 Ma McDermitt volcanic field and on the northeast by the 2.05-Ma-to-present Yellowstone Plateau volcanic field (Fig. 1). Silicic volcanism associated with this province began ca. 16 Ma, with eruptions at the McDermitt caldera complex (Rytuba and McKee, 1984) in northeastern Nevada-southeastern Oregon, and continued as a northeast-moving locus of bimodal volcanism, becoming progressively younger to the northeast (Christiansen and Blank, 1969; Armstrong et al., 1975; Pierce and Morgan, 1992). Rhyolitic rocks include large volumes of densely welded ignimbrites and lava flows with subordinate volumes of nonwelded pyroclastic deposits and smaller volume lava flows. These are the initial products of volcanism (Leeman, 1982), constituting ~85% of the total volcanic material in this province (Leeman, 1982; Christiansen, 1984; Morgan et al., 1984). With the end of rhyolitic activity, tholeiitic lava flows and pyroclastic materials were erupted, thereby concealing the caldera basins and completing the caldera cycle, resulting in the marked lithologically bimodal expression of this volcanic province. Later, additional tholeiitic and more chemically evolved basalts erupted along rift zones perpendicular to the axis of the SRP (Kuntz et al., 1992). The overlying sequence of basalt flows and interbedded alluvial, eolian, and lacustrine sediments thins to the northeast along the axis of the plain (Armstrong et al., 1975, 1980). Faulting and seismicity marginal to the SRP for the last 10 m.y. has an age progression similar to, but slightly in advance of rhyolitic volcanism (Anders et al., 1989; Pierce and Morgan, 1992; Smith and Braile, 1994).

The Heise Group

Four major caldera-forming eruptions occurred within the eastern SRP during the late Miocene and early Pliocene. The calderas and their cogenetic ignimbrites, herein established as the Blacktail Creek Tuff, the Walcott Tuff, the Conant Creek Tuff, and the Kilgore Tuff of the Heise Group, form the framework of a large rhyolitic volcanic field analogous to the present-day Yellowstone Plateau volcanic field. The Heise volcanic field consists of several overlapping or nested calderas that are now buried beneath younger sedimentary and volcanic deposits. Deposits of the Heise Group cover ~35,000 km^2. They are exposed extensively along the margins of the 90-km-wide eastern SRP (Morgan, 1992; Fig. 2). In places, the Heise Group lies stratigraphically below the 2.05-Ma Huckleberry Ridge Tuff erupted from the adjacent Yellowstone Plateau volcanic field (Christiansen, 1984, 2001; Obradovich, 1992). Heise Group rocks lie stratigraphically above tuffaceous sediments of the late Tertiary Medicine Lodge Formation on the northern margin of the plain (Skipp et al., 1979) and above and in places overlapping tuffaceous sediments of the Salt Lake Formation on the southern margin (Allmendinger, 1982; Oriel and Moore, 1985; Love, 1986). Along the northern edge of the SRP, rhyolites from the Heise Group are distributed from the Arco area in the southwest to southern Montana and Big Bend Ridge on the northeast. Along the southern edge of the SRP, rhyolites from the Heise Group are distributed from the American Falls area in the southwest to the Heise–Grand Valley–Palisades Reservoir area in the northeast (Fig. 1). One regional ignimbrite (Kilgore Tuff) from the Heise Group has been recognized as far east as Jackson Hole, Wyoming (Morgan, 1992; Fig. 2A).

In the Heise volcanic field, multiple large-volume rhyolitic ignimbrite sheets are intercalated with locally derived rhyolitic lava flows, nonwelded and welded ignimbrites, and pyroclastic fall, surge, and reworked deposits. Thick rhyolitic ash sequences with distinct SRP-Yellowstone-like geochemistry and ages are present in basins marginal to the SRP and as far away as eastern Nebraska (Izett, 1981; Perkins et al., 1995), Monterey Bay in California (Sarna-Wojcicki, A.M., oral commun., 1998), and the Basin and Range Province (Perkins et al., 1998; Pederson, 1999; Janecke and Evans, 1999).

In ascending order, we recognize four major stratigraphic units from the Heise volcanic field

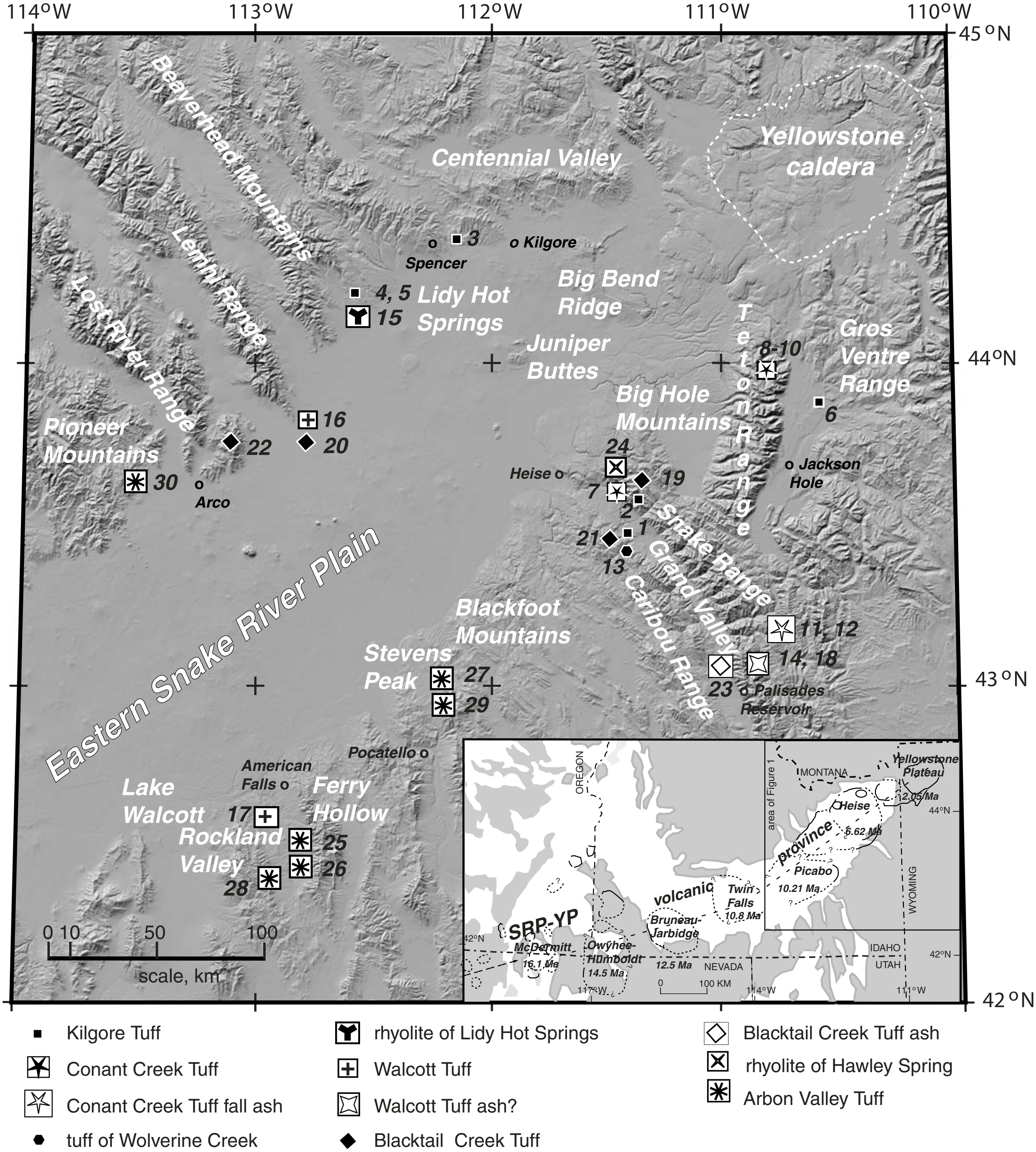

Figure 1. Location map showing a gray-shaded topographic relief image of the eastern Snake River Plain in relation to the Basin and Range province located to the north and south of the plain. To the northeast is the Yellowstone caldera. Sampling locations for units dated in this study are also shown. Sample numbers correspond to numbers in Table 1. Inset in the lower right corner is a generalized topographic index map showing the volcanic fields of the Yellowstone hot spot track, which become progressively younger to the northeast. Areas in white represent elevations <1700 m; areas in gray represent elevations >1700 m. Rhyolitic volcanism associated with a postulated thermal plume (Pierce and Morgan, 1992) began ca. 16.1 Ma at the McDermitt volcanic field in northern Nevada and southeastern Oregon, progressed northeastward forming the eastern Snake River Plain, and arrived at the present position of the Yellowstone Plateau ca. 2 Ma. Dates shown with the volcanic fields represent the inception age of that volcanic field associated with a large-volume caldera-forming eruption (dates for Owyhee-Humboldt volcanic field from Manley and McIntosh, 2004; for Twin Falls volcanic field from Morgan et al., 1997; for Yellowstone Plateau volcanic field from Obradovich, 1992; Christiansen, 2001).

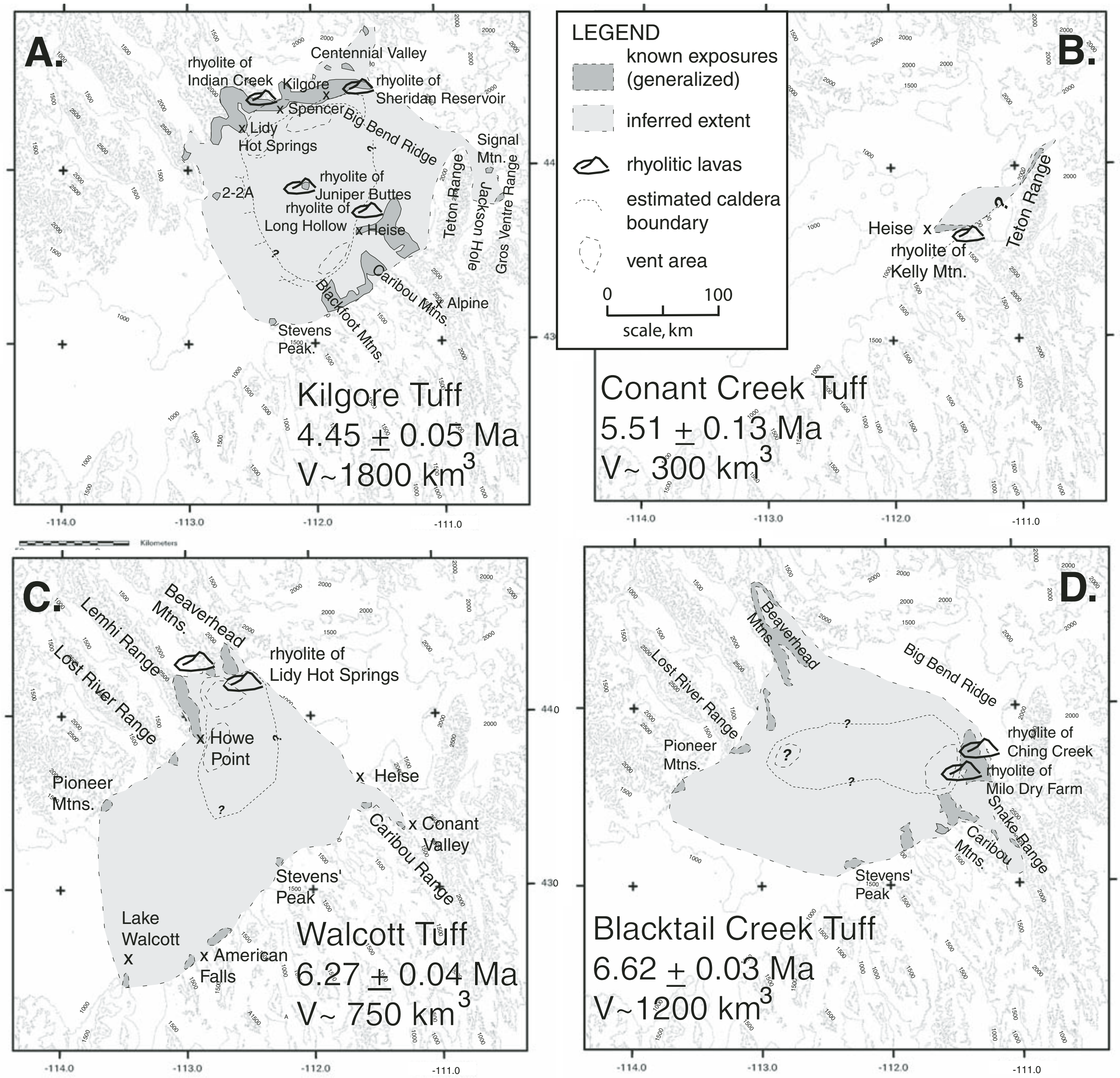

Figure 2. Maps showing the generalized distribution and inferred extent of each of the four major ignimbrites from the Heise volcanic field define the large areal extent of each unit. Exposures of the outflow facies are discontinuous in foothills along the margins of the eastern SRP. Estimated caldera boundaries are shown. Volumes of individual ignimbrite sheets are conservative estimates and roughly calculated as follows: the area of the ignimbrite has been determined on its inferred extent; thicknesses of each ignimbrite are subdivided into extracaldera and intracaldera facies. Average thicknesses for each extracaldera facies are: Kilgore Tuff (50–75 m), Conant Creek Tuff (50 m), Walcott Tuff (50 m), Blacktail Creek Tuff (75 m). Average thickness for each intracaldera facies is conservatively estimated at >1000 m thick. Volumes are considered only as rough estimates. Each caldera is interpreted as a large collapse structure that contains smaller individual eruptive vent areas on the caldera margins. The Kilgore Tuff has been identified in the subsurface of the plain in geothermal well 2-2A.

as the Blacktail Creek Tuff, the Walcott Tuff, the Conant Creek Tuff, and the Kilgore Tuff of the Heise Group. Here, we formally name and give detailed descriptions of the type and reference sections of the Blacktail Creek Tuff and Kilgore Tuff (Appendix 1).[1] Carr and Trimble (1963) describe the type section of the Walcott Tuff. Its reference section is described in Appendix 1. The type and reference sections of the Conant Creek Tuff are described in Christiansen and Love (1978). On the basis of geochemistry, isotopic values, stratigraphic position, mineralogy, paleomagnetism, and isotopic dates, the framework ignimbrites of the Heise Group are correlated between the northern and southern margins of the eastern SRP (Morgan et al., 1984; Morgan, 1992; Fig. 3).

ANALYTICAL METHODS AND RESULTS

$^{40}Ar/^{39}Ar$ dating methods were used to determine eruption ages for regional and local rhyolitic ignimbrites and lava flows exposed in the eastern SRP and for potentially correlative rhyolitic ashes and ignimbrites exposed near Palisades Reservoir, Idaho, and Jackson Hole, Wyoming. Sanidine crystals separated from 26 samples (19 ignimbrites, two lavas, and five fine-grained ash-fall deposits) from eight stratigraphically distinct units were dated by the single-crystal $^{40}Ar/^{39}Ar$ laser-fusion method. For four additional ignimbrite samples with sparse or no sanidine, plagioclase crystals or vitrophyric glass were separated and dated using the bulk-sample resistance-furnace method. Separation, irradiation, and analytical procedures are described in Table 1 and by McIntosh and Chamberlin (1994). Age determination results are summarized in Table 1 and Figures 4, 5, and 6. The complete data set is presented in Appendices 2 and 3 and is available through the GSA Data Repository. Table 2 compares ages obtained in this study with K-Ar and fission-track ages for the large-volume ignimbrites (all errors in this paper are quoted at ± 2σ, even data originally published at ± 1σ). Table 1 and Figure 1 provide specific locations where samples for dating were collected. All ages are calculated relative to Fish Canyon Tuff sanidine monitor at 27.84 Ma (Deino and Potts, 1990), equivalent to Mmhb-1 hornblende at 520.4 Ma (Samson and Alexander, 1987).

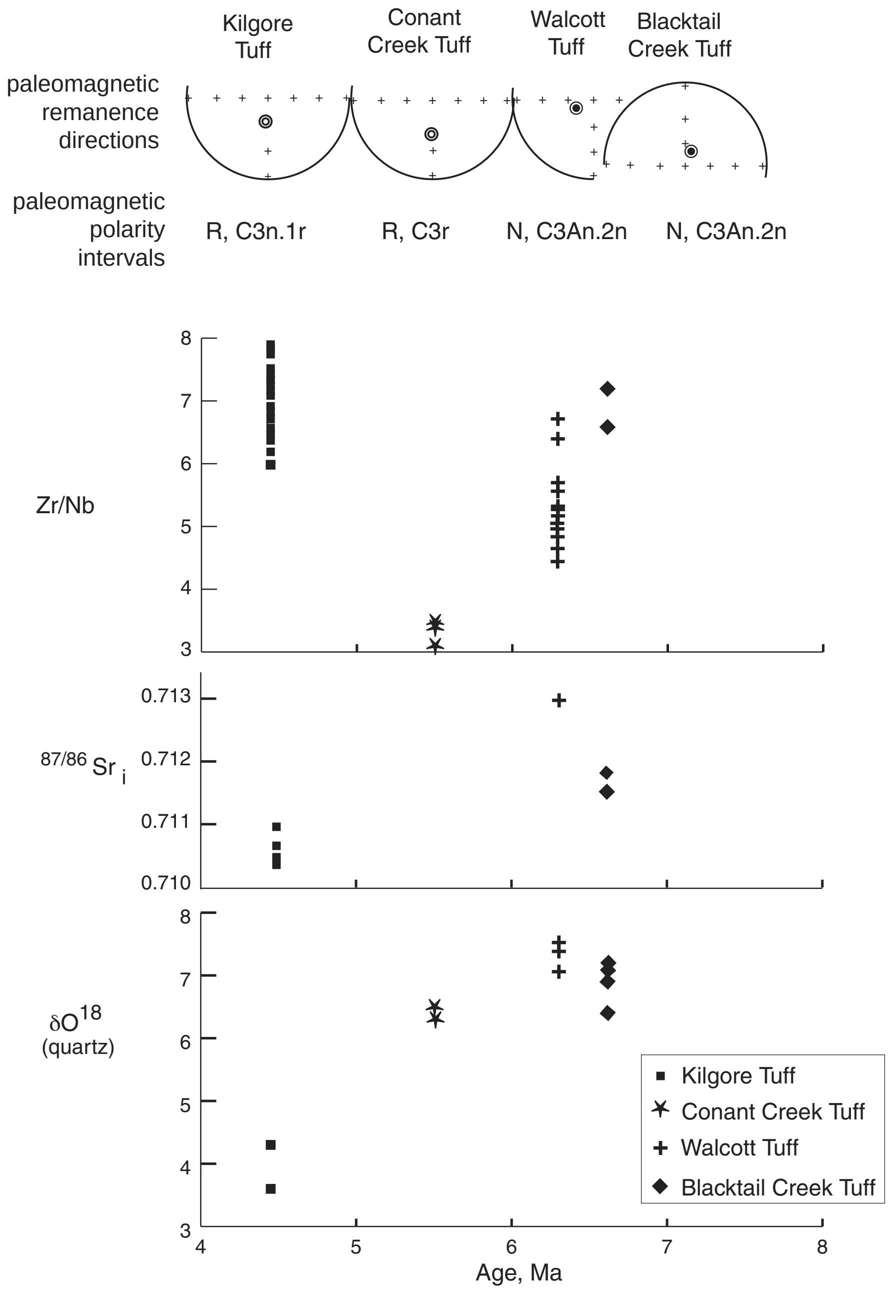

Figure 3. Summary of selected geochemical, paleomagnetic, and isotopic data that help discriminate among the various ignimbrites of the Heise Group (Morgan et al., 1984; Morgan, 1992). Paleomagnetic directions are unit-mean values for each regional ignimbrite. Open symbols represent negative inclinations (reverse polarity) and closed symbols represent positive inclinations (normal polarity).

The single-crystal sanidine analyses have high radiogenic yields (typically 90%–99%) and apparent ages that form tightly grouped, approximately Gaussian distributions (Fig. 5). K/Ca values (Table 1, Fig. 7) are generally consistent among various crystals from individual samples. The K/Ca ratio, calculated from K-derived ^{39}Ar and Ca-derived ^{37}Ar, provides a correlation criterion that can be useful in conjunction with other correlation criteria such as age, lithology, and paleomagnetic direction (McIntosh et al., 1990). Weighted-mean ages and errors were calculated for each sample, after excluding results from a small number of crystals with anomalous ages. In all, data from 15 of the total

[1]GSA Data Repository item 2005059, justification of formal stratigraphic nomenclature and formal stratigraphic descriptions for the type and reference sections of the 6.62 ± 0.03-Ma Blacktail Creek Tuff and 4.45 ± 0.05-Ma Kilgore Tuff, and for the reference section of the 6.27 ± 0.04-Ma Walcott Tuff; results of single-crystal, laser-fusion $^{40}Ar/^{39}Ar$ analyses; results of step-heated, bulk-sample $^{40}Ar/^{39}Ar$ analyses, is available on the Web at http://www.geosociety.org/pubs/ft2005.htm. Requests may also be sent to editing@geosociety.org.

TABLE 1. SUMMARY OF ^{40}AR/^{39}AR RESULTS FOR SANIDINES AND VITROPHYRES FROM RHYOLITES ON THE EASTERN SNAKE RIVER PLAIN AND VICINITY

Sample	No.	Unit	Location (side of plain)	mineral	n	K/Ca	± 2σ	Age (Ma)	± 2σ
ESRP-95–2010	1	Kilgore Tuff	Poplar 7.5′ quad. (S)	Sanidine	13	6.9	7.9	4.43	0.08
ESRP-95–2011A	2	Kilgore Tuff	Hawley Gulch 7.5′ quad. (S)	Sanidine	15	8.9	5.7	4.43	0.04
ESRP-95–2015	3	Kilgore Tuff	Spencer South 7.5′ quad. (N)	Sanidine	14	13.1	11.1	4.44	0.07
ESRP-95–2017B	4	Kilgore Tuff	Lidy Hot Sp. 7.5′ quad. (N)	Sanidine	6	8.1	9.5	4.51	0.05
CSRP-96–94.11	5	Kilgore Tuff	Lidy Hot Sp. 7.5′ quad. (N)	Sanidine	12	10.5	6.5	4.39	0.06
TNP-96–43	6	Kilgore Tuff	Signal Mt. Wyoming (E)	Sanidine	12	9.6	5.8	4.52	0.07
mean age		Kilgore Tuff		Sanidine	6			4.45	0.05
ESRP-95–2013	7	Conant Creek Tuff (“tuff of Elkhorn Spring”)	Hawley Gulch 7.5′ quad (S)	Sanidine	7	8.5	6.4	5.48	0.13
TNP-96–48	8	Conant Creek Tuff	Hominy Peak (N)	Sanidine	7	16.3	10.6	5.57	0.19
TNP-96–48	9	Conant Creek Tuff	Hominy Peak (N)	Vitrophyre*	4	12.4		5.65	0.05
TNP-96–48	10	Conant Creek Tuff	Hominy Peak (N)	Vitrophyre*	4	12.4		5.57	0.09
mean age		Conant Creek Tuff		Sanidine	2			5.51	0.13
TW-96–58b	11	Conant Creek Tuff fall deposit	Palisades Reservoir area (S)	Sanidine	12	6.8	16.8	5.43	0.13
TW-96–58a	12	Conant Creek Tuff fall deposit	Palisades Reservoir area (S)	Sanidine	13	13.7	54.6	5.56	0.08
ESRP-95–2009	13	tuff of Wolverine Creek	Poplar 7.5′ quad (S)	Sanidine	15	1.5	0.4	5.59	0.05
ESRP-95–2017A	15	rhyolite of Lidy Hot Springs	Lidy Hot Sp. 7.5′ quad (N)	Sanidine	13	9.6	4.7	6.20	0.05
ESRP-95–2019B	16	Walcott Tuff	Howe Point (N)	Plagioclase*	8	0.4		6.28	0.05
CSRP-96–76.1	17	Walcott Tuff	Neeley 7.5′ quad (S)	Plagioclase*	11	0.5		6.26	0.05
mean age		Walcott Tuff		plagioclase	2			6.27	0.04
TW-96–65	14	Ash	Palisades Reservoir area (S)	Sanidine	3	5.4	6.6	6.18	0.22
TW-96–66c	18	pumiceous ash	Palisades Reservoir area (S)	Sanidine	7	24.7	11.7	6.35	0.15
ESRP-95–2006	19	Blacktail Creek Tuff	Sticking Springs (S)	Sanidine	14	19.7	3.2	6.60	0.05
ESRP-95–2020	20	Blacktail Creek Tuff	Howe Point (N)	Sanidine	15	18.2	3.8	6.59	0.06
ESRP-95–2001A	21	Blacktail Creek Tuff	Blacktail Reservoir (S)	Sanidine	30	19.4	6.7	6.59	0.04
CSRP-96–97.1	22	Blacktail Creek Tuff	Howe NW 7.5′ quad (N)	Sanidine	15	20.6	1.7	6.64	0.03
mean age		Blacktail Creek Tuff		Sanidine	4			6.62	0.03
TW-96–63a	23	Blacktail Creek Tuff fall deposit	Palisades Reservoir area (S)	Sanidine	11	21.4	4.5	6.54	0.06
ESRP-95–2008	24	rhyolite of Hawley Spring	Heise 7.5′ quad (S)	Sanidine	15	47.2	13.9	7.50	0.04
CSRP-98–127	25	Arbon Valley Tuff	Michaud 15′ quad (S)	Sanidine	15	53.1	14.7	10.22	0.07
CSRP-98–126	26	Arbon Valley Tuff	Michaud 15′ quad (S)	Sanidine	14	59.3	28.8	10.18	0.08
CSRP-98–123a	27	Arbon Valley Tuff	Yandell Spring 15′ quad. (S)	Sanidine	15	81.0	82.0	10.20	0.05
TAV-95.1	28	Arbon Valley Tuff	Rockland East 7.5′ quad. (S)	Sanidine	12	38.5	13.7	10.25	0.03
YS88–801	29	Arbon Valley Tuff	Yandell Spgs. 15′ quad (S)	Sanidine	15	45.2	9.5	10.21	0.05
CSRP-96–100.1	30	Arbon Valley Tuff	Grouse 15′ quad (N)	Sanidine	14	39.3	11.6	10.21	0.03
mean age		Arbon Valley Tuff		Sanidine	6			10.21	0.03

Notes: n—number of individual laser-fused Sanidine crystals used for mean age, or for resistance-furnace-heated vitrophyric glass or plagioclase (denoted by *), number of incremental heating steps in age-spectrum plateau, K/Ca = molar ratio calculated from reactor produced $^{39}Ar_K$ and $^{37}Ar_{Ca}$. Standard deviation of K/Ca (± 2σ) is calculated for single-crystal laser-fusion results. Sample preparation and irradiation: Sanidine was separated by crushing, lithium metatungstate heavy liquid, magnetic separation, and hydrofluoric acid etching. Vitrophyric glass concentrated from sample TW-96-48 by crushing and handpicking. Samples irradiated in machined Al discs for 7 h in D-3 position, Nuclear Science Center, College Station, Texas, along with neutron flux monitor FC-1, Fish Canyon Tuff sanidine, which has an assigned age of 27.84 Ma (Deino and Potts, 1990) equivalent to MMhb-1 at 520.4 Ma (Samson and Alexander, 1987). Instrumentation: Mass Analyzer Products 215–50 mass spectrometer with an automated, all-metal extraction system at New Mexico Geochronology Research Laboratory, Socorro, NM. Individual sanidine crystals (5–30, typically 16, per sample) were fused in vacuum by a 10W continuous CO_2 laser. Reactive gasses were removed for 1–2 min by SAES GP-50 getters operated at 20 °C and ~450 °C. Age calculations: All errors are reported at ± 2σ. Weighted mean ages and errors calculated by inverse variance weighting (Samson and Alexander, 1987). Decay constant and isotopic abundances follow Steiger and Jäeger (1977). See Appendices 2 and 3 on file with the GSA Data Repository. Analytical parameters: Electron multiplier sensitivity averaged 4×10^{-17} moles/pA. System blanks were time-averaged over several analyses. Mean blank values were 78, 1.5, 0.3, 0.8, 1.0×10^{-18} moles (laser) and 1500, 6.7, 1.7, 2.1, 6.6×10^{-18} moles (furnace) at masses 40, 39, 38, 37, 36 respectively. J-factors were determined to a precision of ± 0.2% by CO_2 laser-fusion of 4–6 single crystals from each of 4–6 radial positions around irradiation vessel. Correction factors for interfering nuclear reactions, determined using K-glass and CaF_2, $(^{40}Ar/^{39}Ar)K = 0.0002 \pm 0.0003$; $(^{36}Ar/^{37}Ar)Ca = 0.00026 \pm 0.00002$; and $(^{39}Ar/^{37}Ar)Ca = 0.00070 \pm 0.00005$. Sample locations are detailed in Figure 1 and Appendix 4.

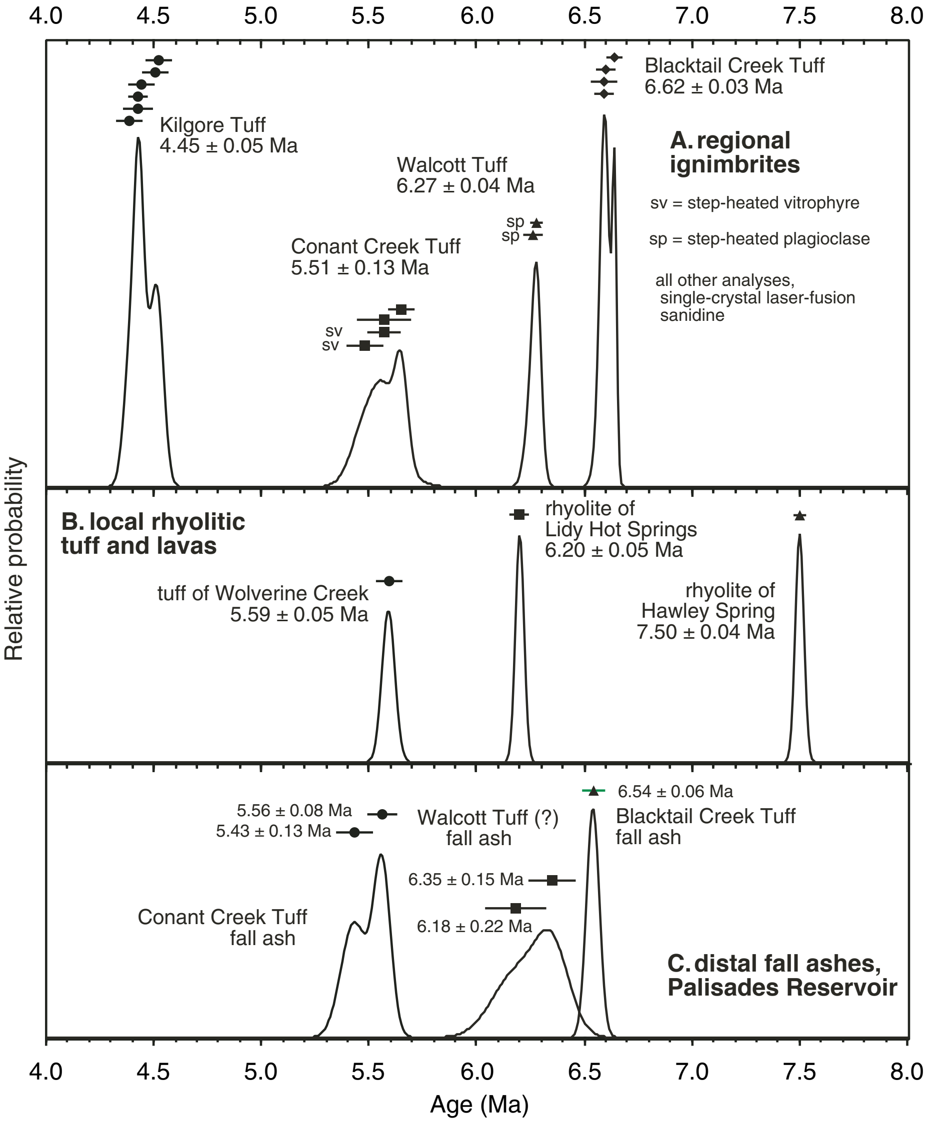

Figure 4. Age probability distribution plots summarizing the $^{40}Ar/^{39}Ar$ dates obtained in this study. (A) Data, including weighted unit-mean ages, from regional ignimbrites erupted from the Heise volcanic field. (B) Data, including weighted unit-mean ages, from minor units in the Heise volcanic field. (C) Data, including individual sample ages, from ashes exposed along the eastern shore of Palisades Reservoir. Each age probability distribution curve (after Deino and Potts, 1992) represents a summation of the Gaussian probability curves for individual age determinations.

257 analyzed crystals were excluded. Of these, 3 dated crystals were anomalously old and are interpreted to represent analyses of xenocrystic feldspars. The remaining 12 rejected single-crystal analyses deviated somewhat from the sample weighted-mean ages and, in most cases, had large analytical uncertainties. Many of these crystals also had small signal sizes, low radiogenic yields, or anomalous K/Ca values; these anomalous age determinations may be due to adhering matrix groundmass or glass, minor alteration, clay formation, or in some cases, may represent partially reset xenocrysts. Weighted-mean ages for the 26 samples dated by single-crystal laser fusion range from 4.5 to 10.2 Ma. Precision values (± 2σ) for the relatively large crystals from ignimbrite samples range between ± 0.03 and ± 0.08 Ma (0.3%–1.8%) (Table 1). Precision values for sanidine from finer-grained fall ashes are somewhat worse, ranging from ± 0.06–0.22 Ma (±0.9%–3.6%) (Table 1).

All four step-heated analyses (two plagioclase separates and two duplicate analyses of one sample of vitrophyric glass) yielded relatively flat age spectra (Fig. 6). For each age spectrum, a plateau age was calculated using three or more contiguous steps that overlap at 2σ and contain at least 50% of ^{39}Ar released. Plateau ages obtained (Table 1) are only slightly less precise than the single-crystal laser-fusion results obtained from sanidine (Figs. 5 and 6). Weighted mean ages for each regional ignimbrite were calculated from the weighted mean ages of ignimbrite samples from that unit (Table 1, Fig. 4). The weighted mean ages of ash-fall samples interpreted to be correlative with the ignimbrites were not used in unit-mean age calculations.

STRATIGRAPHY AND $^{40}AR/^{39}AR$ CHRONOLOGY

Stratigraphic Nomenclature

The stratigraphic nomenclature for the ignimbrite sheets in the Heise Group has evolved in response to advances in understanding of the correlation and distribution of regional units. Mapping on the southern and northern margins of the eastern SRP began at different times and was done by individuals who developed stratigraphic nomenclatures specific to their study areas (e.g., Mansfield and Ross, 1935; Stearns and Isotoff, 1956; Scholten et al., 1955; Staatz and Albee, 1966; Prostka and Embree, 1978; D.J. Doherty, 1981, written commun.; Allmendinger, 1982; McBroome, 1981; Kellogg et al., 1984). McBroome et al. (1981) first suggested that the three extensive ignimbrite sheets on the northern margin of the plain were correlative with the three extensive sheets on the southern margin on the basis of similar ages, mineralogies, stratigraphic positions, and magnetic polarities. Morgan et al. (1984) proposed a new stratigraphic nomenclature in accordance with the North American Stratigraphic Code (North American Commission on Stratigraphic Nomenclature, 1983) based on these similarities and geochemical and isotopic correlations.

Regional Ignimbrites

Arbon Valley Tuff Member of the Starlight Formation

The Arbon Valley Tuff Member of the Starlight Formation (Carr and Trimble, 1963; Kellogg et al., 1994) is well known in the eastern SRP because it is readily identified by abundant crystals of bipyramidal quartz and biotite, a unique mineral assemblage for the eastern SRP-Yellowstone Plateau volcanic province. The prominent ignimbrite is exposed primarily along the southeastern margin of the eastern SRP from Rockland Valley and extends northeast 125 km to the Blackfoot Mountains (Kellogg and

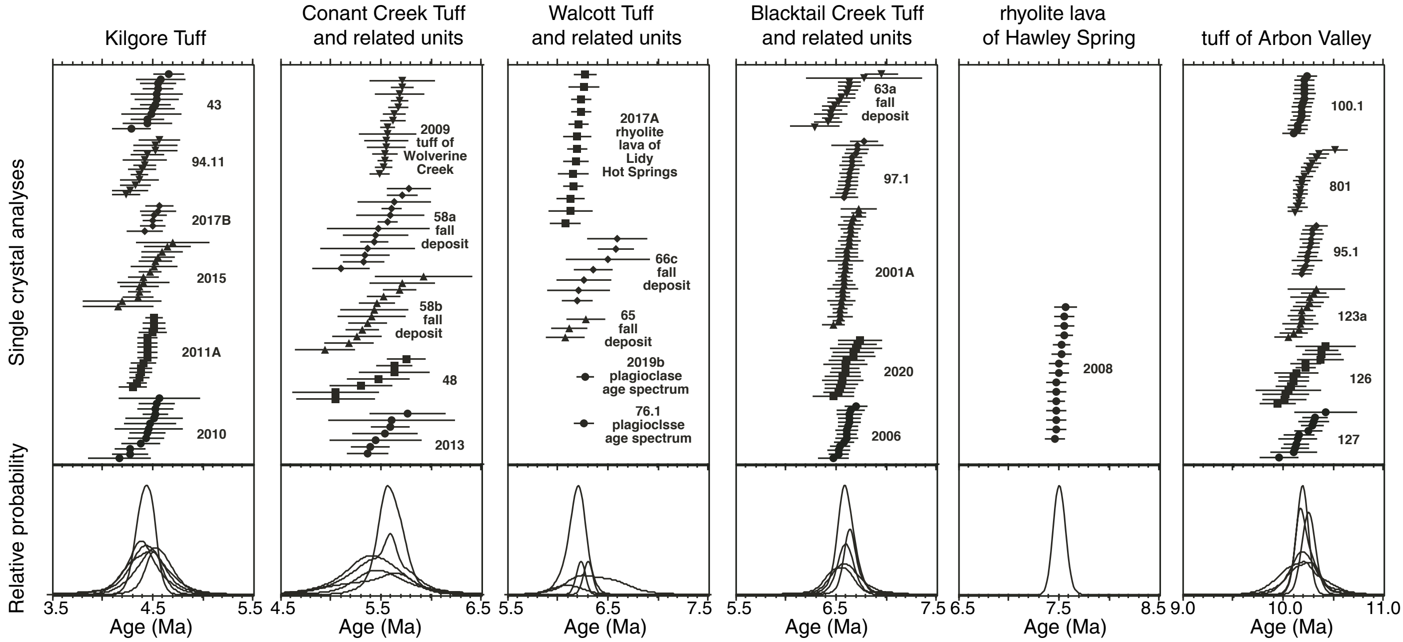

Figure 5. Individual ages and age probability distribution curves for single-crystal laser-fusion analyses, grouped by eruptive unit. Upper panels show ages of individual analyses with 1σ error bars. Samples are identified by the last digits of the sample numbers given in Table 1. Anomalous data excluded from mean calculation, chiefly older grains interpreted as xenocrysts, are not included in this figure. Plateau ages of two samples of step-heated plagioclase from the Walcott Tuff are included for comparison. Lower panels show age probability distribution curves for each sample (after Deino and Potts, 1992).

Embree, 1985; Kellogg et al., 1994). The Arbon Valley Tuff on the northern margin of the plain in the southern Lemhi Range is exposed below a suite of volcanic rocks that includes the Blacktail Creek Tuff and Walcott Tuff. The Arbon Valley Tuff is also exposed in the Pioneer Mountains (B.A. Skipp and S.U. Janecke, oral commun., 1996; Morgan et al., 1997; Fig. 1). Based on its known distribution (Carr and Trimble, 1963; Trimble and Carr, 1976), Pierce and Morgan (1992) suggested the general source location for the Arbon Valley Tuff to be south of the Heise volcanic field in the Picabo volcanic field (Fig. 1 inset). The location of its source was further refined in detailed mapping by Kellogg et al. (1994), who obtained an $^{40}Ar/^{39}Ar$ mean sanidine age of 10.20 ± 0.12 Ma based on three samples. The presence of biotite, a hydrous phase uncommon in other SRP rhyolites, may suggest the Arbon Valley Tuff is more associated with Basin and Range volcanism rather than the SRP. Although the analyses of Kellogg et al. (1994) were performed by step heating of bulk samples, the monitor age used (MMhb-1 at 520.4 Ma) allows direct comparison between their data and the results of our study.

Sanidine from samples of the Arbon Valley Tuff collected at six locations on the northern and southern margins of the eastern SRP yield statistically indistinguishable ages within the 95% confidence level, giving a weighted mean age of 10.21 ± 0.03 Ma (Table 1, Figs. 1, 5, and 8), in excellent agreement with the age determination of Kellogg et al. (1994; Table 2).

Blacktail Creek Tuff

The oldest large-volume (conservative estimate at 1200 km^3) ignimbrite erupted from the Heise volcanic field, formerly referred to as the tuff of Blacktail Creek (Morgan, 1992), is formally named the Blacktail Creek Tuff. We refer the reader to Appendix 1 where the justification for this formal nomenclature is presented. The type section on the southern margin of the plain and the reference section on the northern margin are described in Appendix 1; these two sections represent the lithologic characteristics of the ignimbrite as it typically appears on the northern and southern margins of the eastern SRP.

The Blacktail Creek Tuff is a rhyolitic, densely welded, relatively crystal-rich ignimbrite with 10%–20% total crystals of plagioclase, quartz, sanidine, augite, opaque oxides, and zircon (listed in order of abundance). Exposures are restricted to outflow facies, except near the type section where a thick intracaldera facies is present (Fig. 2D). Along the northern margin of the eastern SRP, the ignimbrite is a simple cooling unit (as defined by Smith, 1960) typically less than 13 m thick. Its thickness varies in relation to the moderate topographic relief on which it was emplaced. The Blacktail Creek Tuff is exposed along the Continental Divide at 2622 m elevation on the Idaho-Montana border in the Beaverhead Mountains and extends as far southwest as the Pioneer Mountains (Skipp et al., 1989). Typically, the base consists of a black or dark brown, densely welded vitrophyre. At several localities, fines-depleted, locally derived, lithic-enriched, ground-layer deposits (cf., Walker et al., 1981) and lithic concentration zones (cf., Sparks et al., 1973) are present in the basal vitrophyre and up into the spherulitic to massive devitrified zones. Above the massive devitrified zone, the unit passes into a zone containing abundant lithophysal cavities. A thin (less than 1 m) capping, pink vitric ash to red platy vitrophyric layer is locally present. We interpret this unit as the fine co-ignimbrite ash elutriated from the top of a pyroclastic flow during emplacement (Morgan, 1988; cf., Sparks et al., 1973; Sparks and Walker, 1977). In many exposures, the ignimbrite rests on an orange paleosol, much of which was wet when incorporated into the pyroclastic flow upon emplacement, as reflected in the abundant white-haloed, rounded, orange lithic clasts in the ignimbrite (McBroome, 1981).

Along the southern margin of the plain, the ignimbrite is well exposed as a simple cooling unit in the foothills of the Big Hole Mountains and in the Snake Range and Caribou Range. Its lithologic characteristics are similar to exposures on the northern margin. On the southern flank of Kelly Mountain in the Big Hole Mountains (Fig. 1, locality 13, Table 2) and along the drainages of Meadow and Willow Creeks in the foothills of the Caribou Range, the southern segments of the Blacktail Creek caldera are, in part, outlined by thick intracaldera facies of the Blacktail Creek Tuff (D.J. Doherty, written commun., 1990). The ignimbrite varies greatly in thickness along the southern margin, ranging from <2 m to >250 m.

Sanidine crystals from samples of the Blacktail Creek Tuff collected at four different locations (Fig. 1) on the northern and southern margins of the eastern SRP yield statistically indistinguishable dates within the 95% confidence level (Table 1, Figs. 4 and 5). The weighted mean age of the Blacktail Creek Tuff is 6.62 ± 0.03 Ma (72 crystals, 4 samples). K/Ca ratios of sanidine from these exposures vary over a narrow range and are distinct from the other ignimbrites in the Heise volcanic field (Fig. 7). Based on the paleomagnetically normal polarity of the Blacktail Creek Tuff, it is likely it erupted during chron C3An.2n of Cande and Kent (1995), although its $^{40}Ar/^{39}Ar$ is slightly older than the 6.269–6.567 Ma age range reported for this normal polarity chron.

The locations of source vents for the Blacktail Creek Tuff are not well known, although the thickness of the unit and coarse size of pumice and crystal fragments in the northern Caribou Range and near Heise on the southern margin of the SRP suggest a nearby vent location. The type section of the ignimbrite is capped by a red, incipiently welded, co-ignimbrite ash containing abundant pumice (<1.2 cm long) and lithic (0.2 cm diameter) clasts. Immediately to the north, a thick intracaldera facies of the Blacktail Creek Tuff is exposed (Fig. 9). Rhyolitic lava flows of similar age are present in this area along a possible ring-fracture zone associated with the Blacktail Creek caldera (D.J. Doherty, 1997, written commun.). These include the rhyolite of Milo Dry Farm and the 6.3 ± 0.3-Ma rhyolite of Ching Creek (Morgan et al., 1984; Figs. 2 and 8). On the northern margin in the Lost River Range, the Blacktail Creek Tuff contains coarse pumice and lithic clasts, possibly also suggesting a second nearby vent location.

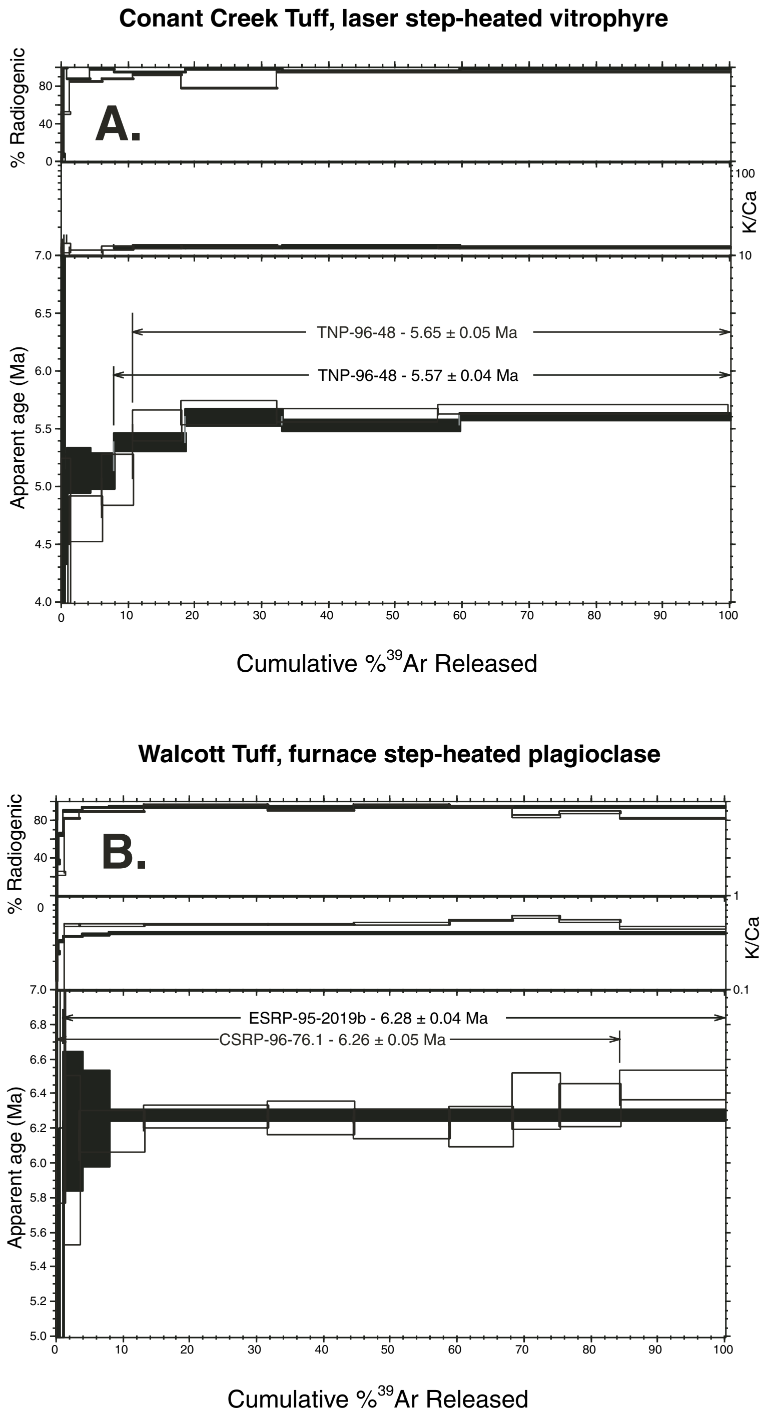

Figure 6. Age spectra for step-heated bulk samples. (A) Results from step-heated vitrophyre from the Conant Creek Tuff. (B) Results from furnace step-heated plagioclase from the Walcott Tuff.

Walcott Tuff

We designate a well-exposed section of the Walcott Tuff in lower Ferry Hollow (Fig. 1) on the southern margin of the eastern SRP (Trimble and Carr, 1976) as the type section for this unit. The reference section for the Walcott Tuff on the northern margin of the eastern SRP in the southern Lemhi Range is described in Appendix 1 (see footnote 1). The type section on the southern margin and the reference section on the northern margin represent the lithologic characteristics of the ignimbrite as it typically appears on the southern and northern margins of the eastern SRP.

The Walcott Tuff is a rhyolitic, densely welded, crystal-poor ignimbrite with less than 2% total crystals of plagioclase, quartz, augite, orthopyroxene, opaque oxides, and zircon. The basal vitrophyre is a black, artifact-quality glass that ranges in thickness from 2 to 50 cm.

TABLE 2. COMPARISON OF RADIOMETRIC AGES OF RHYOLITES FROM THE HEISE VOLCANIC FIELD

Unit	Unit-mean $^{40}Ar/^{39}Ar$ age (Ma)	K/Ar age (Ma)	Fission-track age (Ma)	Reference
Kilgore Tuff	4.45 ± 0.05 (n = 6)	4.1 ± 0.1 (wr)		1
Kilgore Tuff		4.3 ± 0.3 (s)		3
Kilgore Tuff		4.3 ± 0.2 (wr)		4
Kilgore Tuff		4.7 ± 0.1 (?)		1
Kilgore Tuff		4.8 ± 0.3 (s)		5
Kilgore Tuff			4.2 ± 0.3 (z)	2
Kilgore Tuff			4.4 ± 0.4 (z)	3
Kilgore Tuff			4.4 ± 0.6 (z)	3
Conant Creek Tuff	5.51 ± 0.13 (n = 2)		4.3 ± 0.5	6
Conant Creek Tuff		5.99 ± 0.06		7
Walcott Tuff	6.27 ± 0.04 (n = 2)	6.9 ± 0.4 (wr)		1
Walcott Tuff			5.6 ± 0.6 (z)	2
Walcott Tuff		6.0 ± 0.2 (wr)		8
Walcott Tuff		6.3 ± 0.3 (wr)		5
Walcott Tuff		6.5 ± 0.1 (wr)		1
Walcott Tuff		6.5 ± 0.1 (wr)		9
Blacktail Creek Tuff	6.63 ± 0.03 (n = 4)	6.3 ± 0.3 (wr)		10
Blacktail Creek Tuff		6.5 ± 0.1 (wr)		1
Blacktail Creek Tuff		6.5 ± 0.3 (wr)		10
Blacktail Creek Tuff		6.6 ± 0.3 (p)		11
Blacktail Creek Tuff		6.7 ± 0.2 (s)		11
Blacktail Creek Tuff		6.7 ± 0.3 (p)		11
Blacktail Creek Tuff			6.5 ± 0.3 (z)	3
Blacktail Creek Tuff			6.6 ± 0.7 (z)	7

Notes: (wr), K/Ar determinations of whole-rock samples; (s), sanidine phenocrysts; (p), plagioclase phenocrysts; (v), vitrophyre; (z), zircon; (#) refers to specific locations where samples for dating were collected. See Figure 1 for locations. n—number of samples used in unit weighted mean age calculation. All age data are reported at ± 2σ; errors have been doubled for published data with errors originally quoted at ± 1σ. References: 1—Armstrong et al. (1975); 2—McBroome (1981); 3—Morgan et al. (1984); 4—Armstrong et al. (1980); 5—Marvin et al. (1970); 6—Christiansen and Love (1978); 7—Naeser et al. (1980); 8—R.F. Marvin (1986, written commn.); 9—Trimble and Carr (1976); 10—Anders et al. (1989); 11—Kellogg and Marvin (1988).

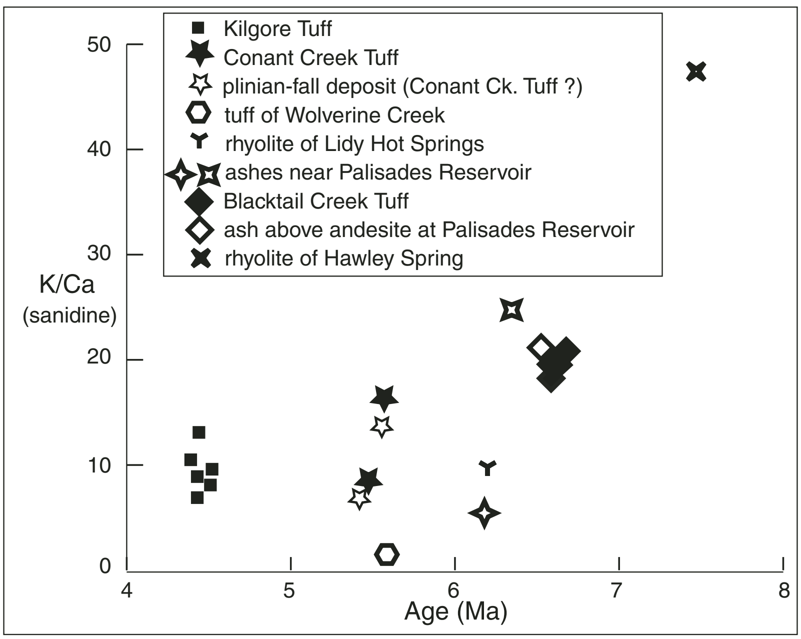

Figure 7. Plot of K/Ca of sanidine versus age of selected units in the Heise Group.

Mansfield and Ross (1935) first noted the Walcott Tuff along the southern margin of the eastern SRP for its remarkable welding zonation. The ignimbrite was originally named and briefly described by Stearns and Isotoff (1956) for an excellent exposure on the east bank of Lake Walcott (Fig. 1). Later, Trimble and Carr (1976) described the unit as two distinct members: a lower bedded tuff and an upper welded ignimbrite. On the basis of its distinct anomalous paleomagnetic direction (Morgan, 1992; Fig. 3), similar trace-element concentrations, isotopic ages, and stratigraphic position, the upper welded ignimbrite member of the Walcott Tuff on the southern margin is correlated with the tuff of Blue Creek on the northern margin. Hence, we refer here to the tuff of Blue Creek as the Walcott Tuff (Morgan, 1988, 1992). Its volume (~750 km^3) is estimated to be less than that of the Blacktail Creek Tuff, based on its distribution and known thicknesses (Fig. 2C).

Exposures on both the northern and southern margins of the eastern SRP are restricted primarily to outflow facies (Fig. 2C). Along the southern margin of the plain, the Walcott Tuff is exposed discontinuously from Lake Walcott northeastward to Stevens Peak near Blackfoot, to the northern side of the Caribou Range. The ignimbrite is an incipiently welded to densely welded unit that has three zones: (1) a basal, dark gray, incipiently welded ash that grades upward into a black vitrophyre which, in turn, grades upward into a perlitic to spherulitic zone; (2) above that, a dark- to medium-gray devitrified ignimbrite that grades upward into a lithophysal zone; and (3) at the top, a red, platy, welded vitric ash that caps the ignimbrite. The thickness of the Walcott along the southern margin varies from 3 m to 10 m.

Along the northern margin of the SRP, the Walcott Tuff is exposed in the foothills of the Pioneer Mountains northeastward to the Lost River and Lemhi Ranges and Beaverhead Mountains (Figs. 1 and 2C). The thickness of the unit ranges here from less than 10 m to as much as 75 m. The Walcott Tuff rests on a bedded pre-ignimbrite ash that grades upward into a distinct, welded, pumice- and ash-fall member of the lower Walcott Tuff. The ignimbrite has a thin, black, densely welded basal vitrophyre overlain by a perlitic to spherulitic glassy zone that grades into a devitrified unit. The thickest part of the ignimbrite is a bluish-gray, platy to lithophysal ignimbrite that has extensive vapor-phase crystallization. A red, co-ignimbrite incipiently welded, vitric ash caps the ignimbrite locally.

Sanidine has not been identified as a crystal phase in the ignimbrite, so plagioclase was used for $^{40}Ar/^{39}Ar$ dating. Plagioclase from samples of the Walcott Tuff collected at two locations

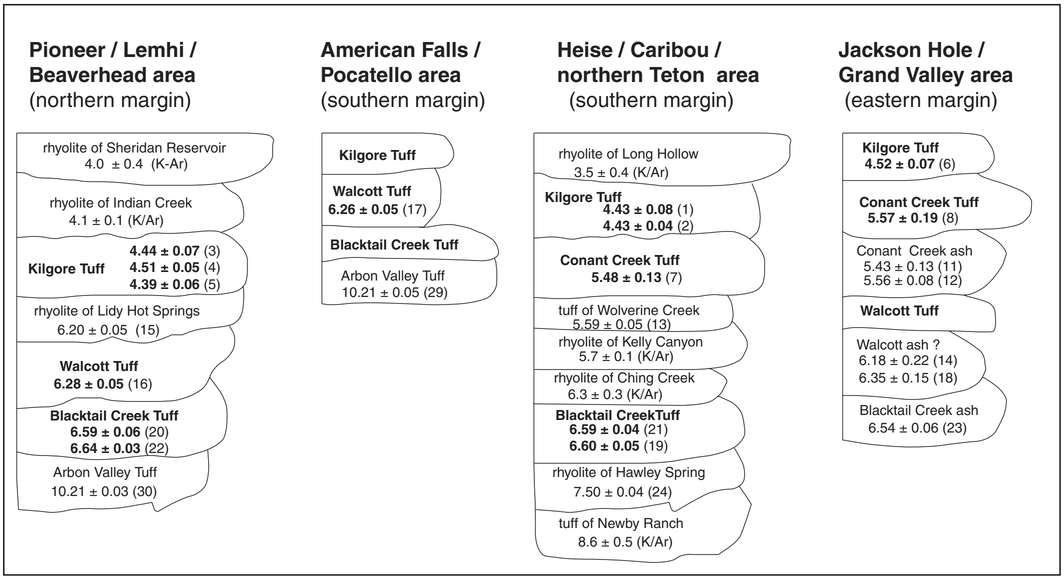

Figure 8. Schematic stratigraphic section of volcanic units exposed along the northern and southern margins of the eastern Snake River Plain. Errors in ages are reported at ± 2σ. Numbers in parentheses correspond to sample localities as shown in Figure 1. K/Ar dates from G.B. Dalrymple and D.J. Doherty as listed in Morgan et al., 1984. Volcanic units shown in bold are the framework ignimbrites of the Heise Group; those shown in plain type are smaller volume units or are not from the Heise Group.

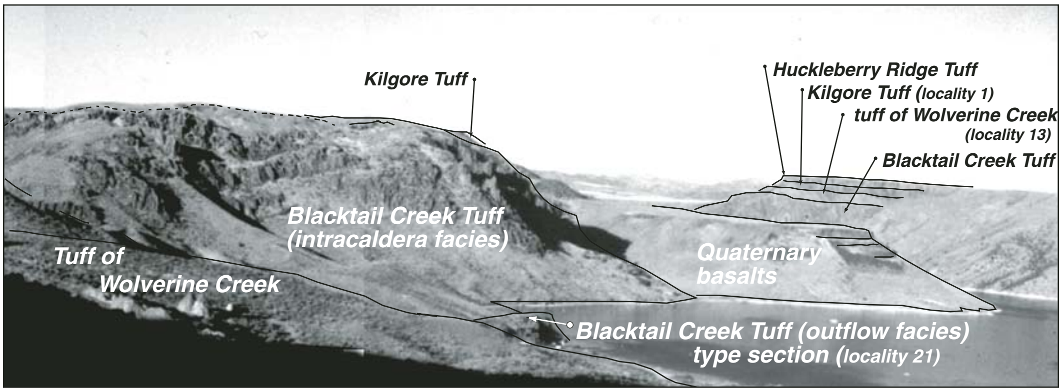

Figure 9. Photograph of volcanic rocks exposed at Blacktail Creek Reservoir. The view is toward the east and shows the thinner type section of the outflow facies of the Blacktail Creek Tuff adjacent to its much thicker, rheomorphically folded, ponded intracaldera facies. See Figure 1 for site locations of localities 1, 13, and 21.

(Fig. 1) on the northern and southern margins of the plain have statistically indistinguishable plateau ages within the 95% confidence level. These samples give a weighted mean age of 6.27 ± 0.04 Ma (Table 1, Figs. 4 and 6B). Based on the paleomagnetically normal polarity of the Walcott Tuff, it is likely it erupted during normal polarity chron C3An.2n (6.269–6.567 Ma) of Cande and Kent (1995).

The location of the eruptive source of the Walcott Tuff, termed the Blue Creek caldera, is not well constrained. An apparent segment of the topographic rim of the Blue Creek caldera is exposed at the southern tip of the Lemhi Range, where a normal fault displaces the outflow facies from the intracaldera facies ignimbrite by ~75 m. On the plainward side of the fault, the Walcott Tuff has been dropped into the eastern SRP and shows extensive rheomorphic deformation. Paleomagnetic studies of flow folds with different orientations show that deformation occurred above the blocking temperatures of iron titanium oxides within the ignimbrite (~570–600 °C; McBroome, 1981). Morgan et al. (1984) describe other evidence for the caldera south of the Lemhi Range. Additional evidence for location of a ring-fracture zone for the Blue Creek caldera along the northern margin of the plain is in the southern Beaverhead Mountains. Here rhyolitic flows and domes in the southern Beaverhead Mountains (Fig. 2C) are similar in age to the Walcott Tuff (McBroome, 1981). One of these, the rhyolite of Lidy Hot Springs, yields a date of 6.20 ± 0.05 Ma (see below). This age is statistically indistinguishable from that of the Walcott Tuff, and we suggest that the flows and domes in the southern Beaverhead Mountains may have erupted near or along a ring-fracture zone of the Blue Creek caldera.

Conant Creek Tuff

Christiansen and Love (1978) first recognized and mapped the Conant Creek Tuff as a widespread Neogene ignimbrite exposed in the northern part of the Teton Range and Jackson Hole, Wyoming. Discontinuous and limited exposures, incomplete stratigraphic sections, and previous difficulties in dating have hampered its regional correlation. Where mapped by Christiansen and Love (1978), the Conant Creek Tuff lies stratigraphically under the 2.05-Ma Huckleberry Ridge Tuff (J.D. Obradovich, 1992; R.L. Christiansen, 2001). Lithologically, the Conant Creek Tuff is a rhyolitic, densely welded, crystal-poor ignimbrite with a nearly aphyric basal vitrophyre. As discussed below, the Conant Creek Tuff is correlated with the tuff of Elkhorn Spring exposed in the Heise area where it forms prominent cliffs. It is a pale blue to grayish blue, densely welded, eutaxitic ignimbrite that grades at its base from conspicuous black, basal vitrophyre upward into a devitrified zone overlain by a lithophysal zone with extensive vapor-phase mineralization. At the base of the ignimbrite, a pink, nonwelded, laminated ash contains abundant elutriation pipes. Its paleomagnetic direction indicates it was erupted during a reverse polarity chron (Morgan, 1992; Fig. 3). Oxygen isotopic analyses of quartz crystals from the Conant Creek Tuff yield a $\delta^{18}O$ value (Morgan, 1992) distinct from those of the Kilgore Tuff (Fig. 3). Trace-element chemistry from selected exposures of the Conant Creek Tuff is also distinct from that of other large-volume, framework ignimbrites of the Heise Group (R.L. Christiansen, written commun., 1988). At present, the Conant Creek Tuff does not appear to be as extensive as the other three ignimbrite sheets in the Heise volcanic field. Known distal exposures of the ignimbrite are in the northern Big Hole Mountains and the northwestern Teton Range (Fig. 2B).

$^{40}Ar/^{39}Ar$ analyses of sanidine crystals from samples of the Conant Creek Tuff collected at two different locations on the eastern margin of the eastern SRP yield a weighted mean age of 5.51 ± 0.13 Ma (Table 1, Figs. 4 and 6A). A vitrophyre collected from the type locality at Hominy Peak (Christiansen and Love, 1978) gave step-heating ages for two samples of 5.57 ± 0.09 Ma and 5.65 ± 0.05 Ma, in excellent agreement with the age of sanidine from the same exposure (Table 2). Previous attempts at dating the Conant Creek Tuff yielded inconsistent results. Whole-rock K-Ar analyses of the basal vitrophyre gave an age of 5.99 ± 0.06 Ma (Christiansen and Love, 1978), yet fission-track analyses of glass gave an age of 4.2 ± 0.7 Ma (Naeser et al., 1980; Table 2). Based on the paleomagnetically reverse polarity of the Conant Creek Tuff, it is likely it erupted during reverse polarity chron C3r (5.230–5.894 Ma) of Cande and Kent (1995).

Christiansen and Love (1978) suggested that the source of the Conant Creek Tuff is in the eastern SRP. Locations of vent sources are unknown at present, although the thickness of the unit is greatest in the Heise cliffs where the ignimbrite is at least 60 m thick. Additional support for volcanic activity in the Heise area at around 5.5 Ma comes from two additional deposits that underlie the Conant Creek Tuff near Heise.

Immediately beneath the Conant Creek Tuff in the Heise cliffs is the previously undated tuff of Wolverine Creek (see discussion below, Fig. 8). Sanidine from the lower member exposed at Meadow Creek Dugway (Fig. 1, locality 13) yielded a weighted mean age of 5.59 ± 0.05 Ma (Table 1, Fig. 4), which is statistically indistinguishable from the 5.51 ± 0.13-Ma age of the Conant Creek Tuff.

The close temporal and spatial relationship between the Conant Creek Tuff and the tuff of Wolverine Creek suggest the tuff of Wolverine Creek may be a precursor or earlier dominantly plinian phase (considering the lower fall-dominated member of the tuff of Wolverine Creek) to the eruption of the Conant Creek Tuff. The thickest known sections of the upper member ignimbrite in the tuff of Wolverine Creek are located in the Heise area and are underlain by a coarse-grained, poorly sorted fall deposit, suggesting a nearby source. Local exposures of ignimbrite units interspersed with alternating coarse and fine ash fall deposits suggest simultaneous eruptions from multiple source vents (Doherty, 1976). In the Heise cliffs, the tuff of Wolverine Creek is exposed directly below the thickest (greater than 75 m) section known at present of the Conant Creek Tuff (Fig. 8).

The other unit exposed below the Conant Creek Tuff that may represent precursor activity preceding the Conant Creek Tuff eruption is the 5.7 ± 0.1-Ma rhyolite of Kelly Canyon (G.B. Dalrymple, written commun., 1979; Morgan et al., 1984; Fig. 8). This rhyolitic lava flow is exposed nearby in the Heise cliff area and gives additional evidence to this area being proximal to a source vent for the Conant Creek Tuff.

Kilgore Tuff

Here, we formally name the youngest large-volume (estimated at >1800 km^3) ignimbrite in the Heise Group as the Kilgore Tuff; justification for the formal nomenclature and descriptions of the type section of the Kilgore Tuff on the northern margin of the plain and reference sections on the northern and southern margins are described in Appendix 1 (see also Fig. 2A).

Lithologically, the Kilgore Tuff is a densely welded, rhyolitic, relatively crystal-poor ignimbrite containing 2%–10% crystals (in order of abundance) of plagioclase, quartz, sanidine, augite, magnetite, and zircon. Lithologic characteristics include abundant, small (1–4 cm diameter) lithophysae concentrated in its upper exposures, maroon pumice present locally, and intermediate phenocryst content with respect to the more crystal-rich Blacktail Creek Tuff and the more crystal-poor Walcott Tuff.

The base of the ignimbrite is exposed in a few places along the northern margin of the eastern SRP where the ignimbrite is a simple cooling unit. An exception is at Lidy Hot Springs where it is buttressed against and overlies the rhyolite of Lidy Hot Springs (Figs. 2A and 8). Most exposures consist only of an upper devitrified platy zone or a well-developed lithophysal zone containing abundant cavities lined with vapor-phase minerals. A vitrophyre formed by welding of a red vitric co-ignimbrite ash containing black or red bubble-wall shards is present in some exposures. The thickness of the Kilgore Tuff varies in relation to the moderate topographic relief on which it was deposited. In most exposures along the northern margin of the eastern SRP, the Kilgore Tuff ranges from <3 m to >120 m in thickness. On the southern margin of the plain, the ignimbrite is less than 11 m thick in most exposures, although at the Heise cliffs it is more than 30 m thick.

Along the southern margin of the eastern SRP, the Kilgore Tuff is a compound cooling unit (cf., Smith, 1960). In some exposures, a coarse pumice-fall deposit underlies the ignimbrite but is separated from the Kilgore Tuff by a soil or thin nonwelded ignimbrite (Morgan, 1988). Typically, the base consists of a thin, dark gray to dark brown, incipiently welded vitric ash passing up into a black, densely welded basal vitrophyre. At several localities, fines-depleted, locally derived, lithic-enriched ground-layer deposits (cf., Walker et al., 1981) and lithic concentration zones containing locally derived lithic clasts are present near the top of the basal vitrophyre and up into the spherulitic to massive devitrified zones. Above the massive devitrified zone, the unit typically passes into a zone containing abundant lithophysal cavities. The compound cooling nature of the ignimbrite is demonstrated by a repetition of massive or platy devitrified zones overlain by lithophysal zones. This sequence in some cases is repeated several times in a single exposure, also producing distinctive oscillatory zonation in trace element composition. Locally, abrupt changes in the size of lithophysal cavities are present. A pink vitric ash to red platy vitrophyre <1 m thick caps the ignimbrite and is interpreted as the fine co-ignimbrite ash elutriated from the top of the pyroclastic flow during emplacement (Morgan, 1988).

Along the northern margin of the eastern SRP, the Kilgore Tuff is exposed north of the Centennial Valley of Montana to the Kilgore area and extends to the southern Beaverhead Mountains. Along the southern margin, the ignimbrite is exposed in the Big Hole Mountains and the Caribou Range and extends to the Blackfoot Mountains (Fig. 1). As discussed below, the Kilgore Tuff extends as far east as Jackson Hole, Wyoming. Within the eastern SRP, the ignimbrite has been recognized in drill holes (Doherty, 1979; Embree et al., 1978) and is also exposed at Juniper Buttes (Morgan, 1988; Figs. 1 and 2A).

Sanidine crystals from samples of the Kilgore Tuff collected at six different locations (Figs. 1 and 8) on the margins of the eastern plain have statistically indistinguishable dates (Table 1, Fig. 5). The weighted mean of these dates is 4.45 ± 0.05 Ma. The K/Ca ratios of sanidine from these six samples are nearly identical and are distinct from some of the other ignimbrites in the Heise Group (Fig. 7). Based on the paleomagnetically reverse polarity of the Kilgore

Tuff, it is likely it erupted during reverse polarity chron C3n.1r (4.290–4.480 Ma) of Cande and Kent (1995).

The Kilgore Tuff probably was erupted from multiple, widely separated source vents (Morgan, 1988). Locations of two vent source areas are inferred to be on the northern margin near Spencer and Lidy Hot Springs; a third source area is on the southern margin near Heise (Fig. 1). Evidence for proximity to source vents at these locations includes results from magnetic fabric analyses, abrupt lateral changes in the size of pumice and lithic clasts within short distances, and the rapid increase in the unit's thickness at these sites. Near Spencer, extensive elutriation pipes are associated with rheomorphic features and faults where deformation occurred at elevated temperatures (i.e., 570–600 °C) in response to caldera collapse. The proposed vent locations on the north side of the plain coincide with local Bouguer gravity lows (Morgan, 1988). Four rhyolitic lava flows with K/Ar ages similar to the $^{40}Ar/^{39}Ar$ mean age of the Kilgore Tuff may be related to the Kilgore caldera (Figs. 2A and 8). The 4.14 ± 0.09-Ma rhyolite of Indian Creek (G.B. Dalrymple, written commun., 1979) near Lidy Hot Springs, the 4.0 ± 0.4-Ma rhyolite of Sheridan Reservoir near Kilgore (D.J. Doherty, written commun., 1983; Morgan et al., 1984), and the 3.5 ± 0.4-Ma rhyolite of Long Hollow north of Heise and in the Sugar City well (D.J. Doherty, written commun., 1983; Embree et al., 1978; Morgan et al., 1984) are located in areas that may be on the ring-fracture zone of the Kilgore caldera. A fourth rhyolitic lava flow is present at Juniper Buttes in the center of the eastern SRP (Fig. 2A) and has K/Ar ages of 3.31 ± 0.06 Ma, 3.47 ± 0.06 Ma, and 3.72 ± 0.08 Ma (G.B. Dalrymple, written commun., 1988). Quartz phenocrysts from these four lava flows have $\delta^{18}O$ values that are similar to the Kilgore Tuff and distinct from the other regional ignimbrites in the Heise Group (Morgan, 1988). The age of rhyolites at Juniper Buttes, the presence of the Kilgore Tuff at Juniper Buttes, and the central location of this dome complex relative to the inferred buried vents indicate that Juniper Buttes is a relatively young rhyolitic feature, and is a likely resurgent dome or upfaulted block associated with the Kilgore caldera (Morgan, 1988). Rectilinear fault patterns at Juniper Buttes (Fig. 10; Kuntz, 1979) are very similar to those described for resurgent domes elsewhere (e.g., Timber Mountain Dome—Smith and Bailey, 1968; Byers et al., 1976; Redondo Dome in the Valles caldera—Smith and Bailey, 1968; Nielsen and Hulen, 1984; and Yellowstone—Christiansen, 1984; U.S. Geological Survey, 1972).

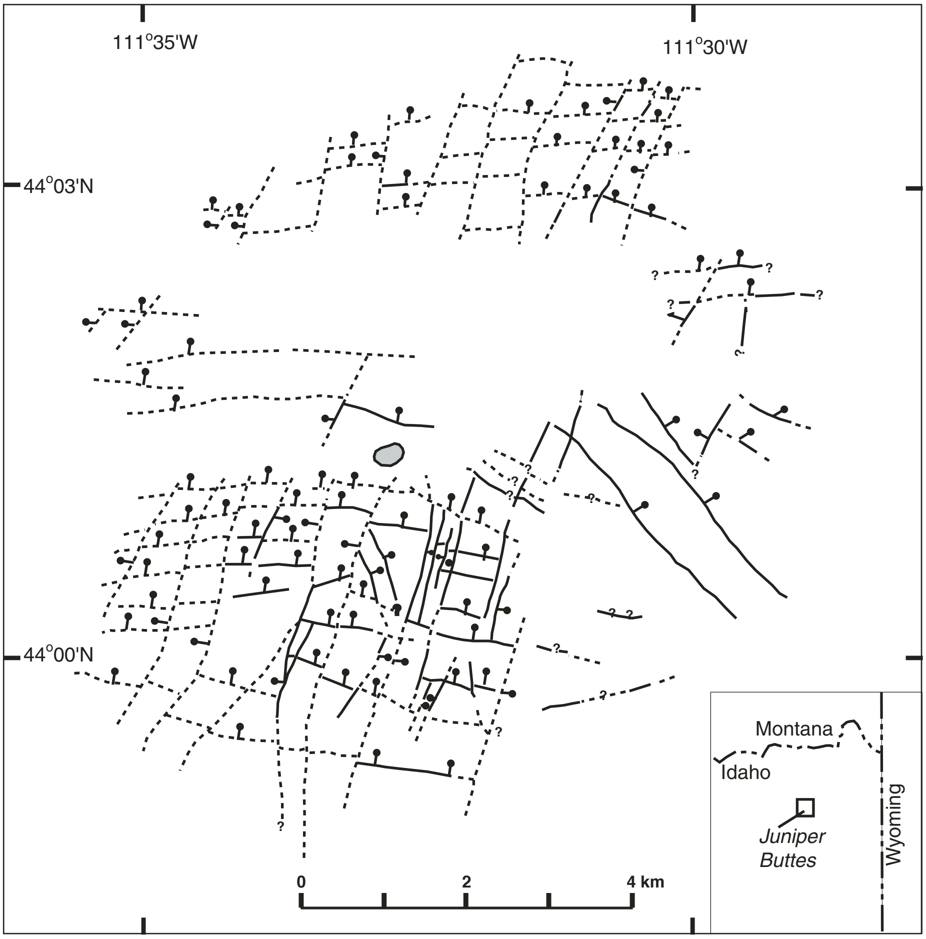

Figure 10. Rectilinear fault patterns present at the Juniper Buttes complex (modified after Kuntz, 1979). The stippled area near the center represents the area where the Kilgore Tuff is exposed.

Local Rhyolitic Units in the Heise Group

Rhyolite of Hawley Spring

Some of the oldest rhyolites erupted from the Heise volcanic field are exposed along the southern margin of the eastern SRP in the Heise cliffs. The rhyolite of Hawley Spring overlies the tuffaceous lacustrine sediments of the tuff of Newby Ranch and underlies the 6.62 ± 0.03 Ma Blacktail Creek Tuff (Fig. 8). This medium brown to gray or lavender, mostly devitrified, porphyritic, massive, thick (0–140 m) rhyolite flow contains abundant quartz, sanidine, plagioclase, and minor amounts of biotite and hornblende (Prostka and Embree, 1978). The unit forms the prominent lower cliffs above the town of Heise where vertical and folded columnar joints, flow margins, and crumble breccia are well exposed. The flow is hydrothermally altered and punky along major fractures and fault zones where abundant iron-oxide staining is present. The base of the flow is laminated. A K-Ar age of 7.2 ± 0.1 Ma was reported by Morgan et al. (1984) for sanidine from this unit. In this study, sanidine from fifteen crystals from one sample of the rhyolite gave a weighted mean age of 7.50 ± 0.04 Ma (Table 1, Fig. 4).

Tuff of Wolverine Creek

Also exposed in the Heise cliffs and in the Heise area is the tuff of Wolverine Creek, typically forming softly rounded hills and gentle slopes (Prostka and Embree, 1978). The tuff of Wolverine Creek can be divided into two members. (1) The lower and thicker unit is light gray to yellowish gray, obsidian-bearing, crystal-poor, and pumiceous. It contains nonwelded to moderately welded rhyolitic ignimbrites and planar to cross-bedded, locally massive, pumiceous, obsidian-bearing, vitroclastic rhyolitic fall and surge deposits. Sanidine from one sample (n = 15 crystals) in this lower member yielded a weighted mean age of 5.59 ± 0.05 Ma (Table 1, Fig. 4). (2) The upper unit is an orange to pinkish gray, crystal-poor, nonwelded to slightly welded rhyolitic ignimbrite with vapor-phase recrystallization. It contains sparse crystals, including plagioclase, augite, sanidine, brown hypersthene, and trace amounts of magnetite and zircon (Doherty, 1976).

As described by Doherty (1976), the tuff of Wolverine Creek is a pyroclastic deposit of limited extent. It is confined to the southern margin of the eastern SRP in the northern Big Hole Mountains, the Caribou Range, the Blackfoot Mountains, and the Snake River graben between the Caribou Range and Big Hole Mountains. It is well exposed in the Heise cliffs (Fig. 8) and at Blacktail Reservoir (Fig. 9) and along Meadow Creek in the northern Caribou Range. Doherty (1976) describes a sequence of base-surge deposits within the tuff of Wolverine Creek along Meadow Creek Canyon that is interspersed with nonwelded ignimbrite and ash- and pumice-fall deposits. Thick ash beds with alternating coarse layers of pumice and finer ash are present throughout the northern Caribou Range and Big Hole Mountains. The tuff of Wolverine Creek varies in thickness from several meters to ~300 m.

Rhyolite of Lidy Hot Springs

The rhyolite of Lidy Hot Springs is exposed locally along the northern margin of the eastern SRP in the southern Beaverhead Mountains near Lidy Hot Springs (Figs. 1, 2C, and 8). Lithologically, the unit is a perlitic to spherulitic, phenocryst-poor rhyolite lava flow that is well exposed in a roadcut on Idaho State Highway 22 below the 4.45-Ma Kilgore Tuff (Fig. 1, locality 15). Mineralogically it contains sparse tiny phenocrysts of sanidine and quartz. The rhyolite has highly contorted flow banding with alternating perlitic and devitrified layers. Spherulites up to 10 cm in diameter are present. Its known distribution is limited to this single exposure.

Sanidine from one sample of the rhyolite of Lidy Hot Springs gave an $^{40}Ar/^{39}Ar$ date of 6.20 ± 0.05 Ma (n = 13 crystals; Fig. 4, Table 1), significantly older than the previously published K-Ar date of 5.4 ± 0.1 Ma (from G.B. Dalrymple, written commun., 1979, in Morgan et al., 1984). The $^{40}Ar/^{39}Ar$ date is statistically indistinguishable from the 6.27 ± 0.04 Ma value for the Walcott Tuff, supporting the interpretation that the two units are related (Morgan et al., 1984). The rhyolite of Lidy Hot Springs may be located near a ring-fracture zone of the Blue Creek caldera, source of the Walcott Tuff.

Distal Correlative Units of the Heise Volcanic Field

Stratigraphic Relationships Among the Conant Creek Tuff, Kilgore Tuff, and Tuff of Elkhorn Spring

$^{40}Ar/^{39}Ar$ dates, together with paleomagnetic, trace element, mineralogical, and stratigraphic position data, have helped to establish accurate correlations between distal and proximal facies of Heise Group ignimbrites. These correlations clarify stratigraphic relationships among the ignimbrites originally mapped as the Conant Creek Tuff, Kilgore Tuff, and tuff of Elkhorn Spring. Christiansen and Love (1978) originally applied the name "Conant Creek Tuff" to what they interpreted as a widespread ignimbrite underlying the 2.05-Ma Huckleberry Ridge Tuff (Christiansen, 2001) in the northern Teton Range and Jackson Hole, Wyoming. This "Conant Creek Tuff" is in reality two different ignimbrite sheets, erupted during widely separated events, the first at 5.51 Ma and the second at 4.45 Ma.

Most of the "Conant Creek Tuff" identified by Christiansen and Love (1978) and mapped by Love et al. (1992) in Jackson Hole, Wyoming, is actually a distal facies of the 4.45-Ma Kilgore Tuff. Distal facies Kilgore Tuff extends as far east as the Gros Ventre Range. A $^{40}Ar/^{39}Ar$ date of 4.52 ± 0.07 Ma was determined for the ignimbrite underlying the 2.05-Ma Huckleberry Ridge Tuff at Signal Mountain, Grand Teton National Park, Wyoming; its age is statistically indistinguishable from ages determined for the Kilgore Tuff at five other localities (Figs. 1, 4, and 5).

The remainder of the "Conant Creek Tuff" of Christiansen and Love (1978) is a 5.5-Ma ignimbrite correlative with an ignimbrite exposed in the Heise area, formerly termed the "tuff of Elkhorn Spring" (Fig. 1, locality 7; Morgan and Bonnichsen, 1989). The older ignimbrite includes Christiansen and Love's (1978) type section Conant Creek Tuff at Hominy Peak in the northwestern Teton Range, which we have dated here as 5.57 ± 0.19 Ma by $^{40}Ar/^{39}Ar$ on sanidine. This age overlaps with the 5.48 ± 0.13-Ma age determined from the "tuff of Elkhorn Spring" in the Heise area. Additional support for the correlation between the Conant Creek Tuff at Hominy Peak and the "tuff of Elkhorn Spring" exposed in the Heise cliffs comes from trace-element and isotopic chemistry and paleomagnetic data (Morgan, 1992; Fig. 3). Both contain a distinctive green pyroxene not found in the three other large-volume ignimbrites of the Heise Group (D.J. Doherty, written commun., 1988). We propose that the name Conant Creek Tuff be applied to the 5.51-Ma ignimbrite exposed near Heise and at Hominy Peak and that the name "tuff of Elkhorn Spring" be abandoned.

Correlations Between Regional Ignimbrites and Distal Fall Deposits Near Palisades Reservoir

A thick series of rhyolitic ash-fall, tuffaceous lacustrine, and plinian-fall deposits are exposed 50 km east of the Heise cliffs along the Grand Valley fault (Anders et al., 1989) near the eastern and northeastern edge of Palisades Reservoir (Figs. 1 and 11; localities 11, 12, 14, 18, 23). Several of these ash deposits can be correlated with some of the regional ignimbrites from the Heise volcanic field using $^{40}Ar/^{39}Ar$ dates and the chemistry of sanidine crystals. Fall deposits from the Blacktail Creek and Conant Creek eruptions are confidently identified (Table 1, Fig. 3).

Along the eastern shore of Palisades Reservoir (Figs. 1 and 11, locality 23), fine-grained ashes overlie a 6.8-Ma andesite (Oriel and Moore, 1985). Sanidine collected from an ash bed at this locality gives an $^{40}Ar/^{39}Ar$ date of 6.54 ± 0.06 Ma (Fig. 4), statistically indistinguishable from the 6.62 ± 0.03-Ma mean age of the Blacktail Creek Tuff. Its source is estimated to be ~60 km to the west in the Heise volcanic field. Similar K/Ca ratios of sanidine further support the correlation between this ash and the Blacktail Creek Tuff (Fig. 7).

Also present at several localities along the eastern shore of Palisades Reservoir is a fine-grained, well-sorted, bedded ash-fall deposit (Figs. 1 and 11, locality 14). Sanidine from this ash at one location gave a weighted mean $^{40}Ar/^{39}Ar$ age of 6.18 ± 0.22 Ma (n = 3 crystals; Table 1). Zircon crystals from this same ash bed gave fission-track dates of 7.07 ± 0.44 and 6.68 ± 0.40 Ma (Oriel and Moore, 1985). Sanidine from an ash bed at a second location (Figs. 1 and 11, locality 18) gave an $^{40}Ar/^{39}Ar$ date of 6.35 ± 0.15 Ma (n = 7 crystals; Table 1) that is statistically indistinguishable at the 2σ level. As discussed below, the age of ash at locality 18 has implications for the timing of movement of an overlying limestone slide block. Dates from sanidine crystals from both localities 14 and 18 are similar and are statistically indistinguishable from the 6.27 ± 0.04-Ma mean age of the Walcott Tuff. However, although both ash beds contain sanidine, no sanidine has been found in the plagioclase-bearing Walcott Tuff. Sanidine in the ash beds is of low concentration and may have been produced by the initial eruptions of the upper fractionated parts of the Walcott Tuff magma chamber. Alternatively, the 6.18 ± 0.22 Ma and 6.35 ± 0.15 Ma ashes may be related to smaller volume explosive rhyolitic eruptions from the Heise volcanic field. These units are similar in age to rhyolites from Borehole WO-2, which gave $^{40}Ar/^{39}Ar$ ages of 6.12 Ma and 6.38 Ma (Anders et al., 1997; no errors reported). Anders et al. (1997) identified the 6.38 Ma unit as the tuff of Wolverine Creek. We consider this unlikely given the precisely determined 5.59 ± 0.05-Ma age of the tuff of Wolverine Creek obtained from sanidine at its type locality in this study. A recent examination of WO-2 by the authors and W.R. Hackett indicate the 6.38-Ma unit in Borehole WO-2 is

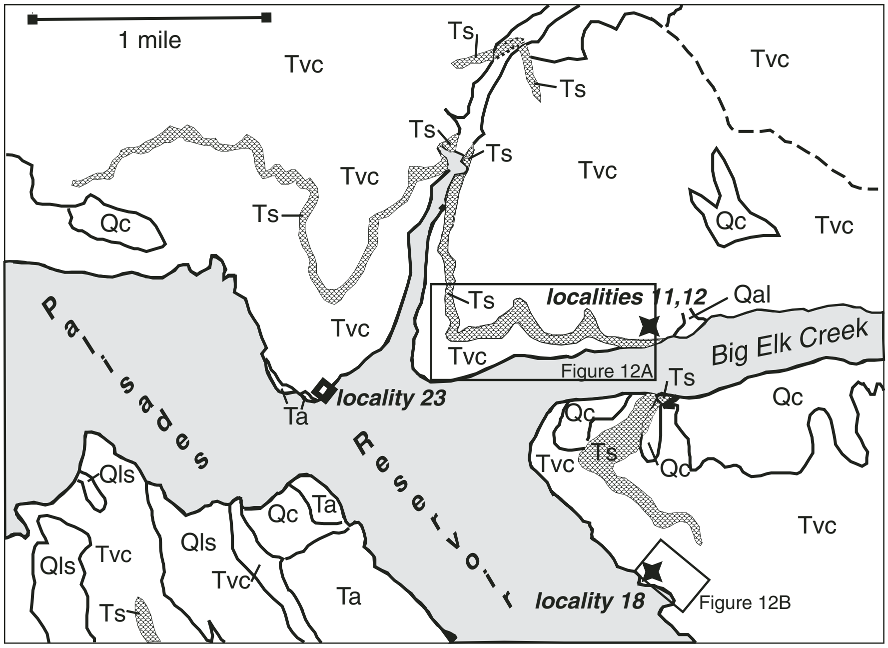

Figure 11. Modified geologic map showing relationship of detachment slide blocks (Ts) with Tertiary volcaniclastic sediments (Tvc) at Palisades Reservoir (see Fig. 1; from Oriel and Moore, 1985). The slide blocks are limestone of the Mississippian Mission Canyon Formation that slid from the Snake Range into a basin accumulating Miocene volcaniclastic sediments. Isotopic ages from ashes bounding the slide blocks provide precise limits for the age of deformation as described in the text. Other symbols on map include Quaternary colluvium (Qc), Quaternary alluvium (Qal), Quaternary landslide deposits (Qls), and Tertiary andesite (Ta). Locality 14 is ~2 km southeast of locality 18. Locations of Figures 12A and 12B are also shown. Sample location sites from Table 1 are shown.

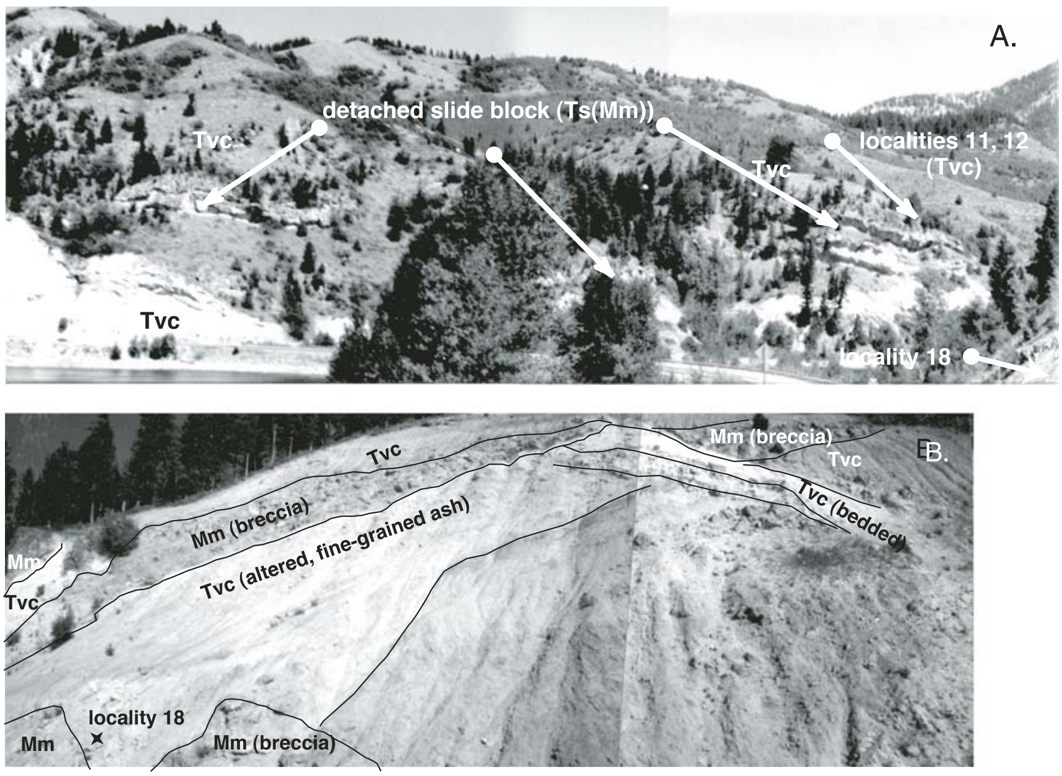

Figure 12. (A) Photo of slide block (Ts) bounded by Miocene volcaniclastic sediments along east side of Palisades Reservoir. Localities 11, 12, and 18 are also shown. Locality 14 is ~2 km southeast of locality 18. See Figure 11 for location of photo. (B) Photo of chaotic breccia. Symbols include Tertiary volcaniclastic sediments (Tvc), Tertiary slide blocks (Ts), and Mississippian Mission Canyon Formation (Mm).

not an ignimbrite but rather a rhyolite lava flow. Possibly, the initial explosive eruptions that are related to emplacement of the 6.38 Ma rhyolite present in WO-2 produced some of the ash beds now exposed near Palisades Reservoir.

Two age determinations from sanidine crystals in a 7-m-thick plinian-fall deposit exposed along a roadcut next to Elk Creek near Palisades Reservoir (Figs. 1, 11, and 12, localities 11, 12) have weighted mean ages of 5.56 ± 0.08 Ma (n = 13 crystals) and 5.43 ± 0.13 Ma (n = 12 crystals). These values are statistically indistinguishable from the 5.51 ± 0.13-Ma weighted mean age of the Conant Creek Tuff (Table 1, Fig. 5). Correlation between the plinian-fall deposit and the Conant Creek Tuff is further supported by similarity in K/Ca ratios of the sanidine crystals (Fig. 7).

TIMING OF TECTONIC EVENTS

Seismically Triggered Slide Blocks

Some of the ash deposits along the northeastern edge of Palisades Reservoir described above overlie or underlie large blocks of Cambrian to Mississippian rocks that were inferred by Oriel and Moore (1985) to have slid from the crest and southwest flank of the Snake Range. Some of these blocks are kilometers in length and several tens to a few hundred of meters in thickness. Explanations for the duration and causal mechanism of the massive slide block movement are controversial (Moore et al., 1987; Anders, 1990; McCalpin et al., 1990; Boyer and Hossack, 1992). Whereas Oriel and Moore (1985) inferred that these slide masses moved from the crest and southwest flank of the Snake Range, they did not propose a triggering mechanism for such large detachments. Boyer and Hossack (1992) inferred that these slide blocks were emplaced over a relatively long time and "crept" into place. They interpreted this from lithologic characteristics within various slide blocks mostly along the Grand Valley Fault and the contact between them and the underlying blocks. They also recognized, however, a possibility that some of these blocks may have been emplaced catastrophically. Other researchers cite evidence that suggests rapid catastrophic emplacement for specific blocks in this area (Moore et al., 1987; Anders, 1990; McCalpin et al., 1990).

Dated ashes from this study that are exposed below and above one of these slide blocks allow the timing of movement at this site to be assessed. The Mississippian Mission Canyon Limestone is underlain by a fine ash and directly overlain by a 7-m-thick plinian-fall deposit (localities 11, 12, Figs. 11B and 12A). Along its length, the detachment block ranges in thickness from 10 to 50 m, is 3 km long, and is relatively coherent. Locally the lower 2–3 m of the limestone block is extensively jointed and fractured. The block rests on a matrix-supported chaotic breccia containing limestone clasts as large as 3 m in diameter in an ash-rich matrix that shows some hydrothermal alteration. The underlying volcaniclastic sediments show soft-sediment deformation.

Ash deposits above the block include a 7-m-thick plinian-fall deposit resting immediately above the slide mass, in turn overlain by a 1- to 2-m-thick sequence of fine-grained ashes interlayered with shard-rich marlstone units, which locally show reworking, discontinuous bedding, and soft-sediment deformation. The 7-m-thick plinian-fall deposit consists of alternating beds of coarse ash and fine ash that become somewhat coarser and more lithic-rich upward in the section. Near the top of the 7-m-thick section, the ash is poorly sorted and coarse and contains ~40% pumice fragments up to 5 cm in diameter and ~20%–30% subangular lithic clasts up to 1.5 cm in diameter. Individual ash layers range in thickness from 1 to 2 cm to 50 cm, averaging ~30 cm thick. There is no evidence for erosion between individual ash beds, suggesting the fall deposit may have been produced by a single eruptive event. Variations in grain size are typical for primary fall deposits and may relate to changes in intensity of the eruption, physical changes in the vent, or variations in wind patterns (Fisher and Schmincke, 1984).

To bracket the timing of the slide block emplacement, ash and pumice samples were collected below and above this slide block. Sanidine from the underlying ash gave single crystal dates of 6.18 ± 0.22 Ma and 6.35 ± 0.15 Ma (Table 1), supporting correlation with the 6.27 ± 0.04-Ma Walcott Tuff as previously discussed. Sanidine from samples collected 6 m and 1 m above the base of the 7-m-thick plinian-fall deposit, which overlies the limestone block, yielded ages of 5.56 ± 0.08 Ma and 5.43 ± 0.13 Ma, respectively. These ages support the interpretation that the plinian-fall deposit occurred from a single eruptive event and suggest that it correlates with the 5.51 ± 0.13-Ma Conant Creek Tuff (Table 1, Figs. 4 and 6A). These results indicate that the limestone detachment block along the northeastern margin of Palisades Reservoir must have moved into place between 6.3 Ma and 5.5 Ma. The nature of the chaotic breccia with incorporated ash matrix beneath the detachment block suggests that the rock mass moved catastrophically onto unconsolidated volcaniclastic sediments. Given that a coarse, thick plinian-fall deposit related to eruption of the Conant Creek Tuff immediately overlies the slide block, we consider it possible that catastrophic movement of the slide block was seismically triggered during the caldera eruption of the Conant Creek Tuff 50 km west in the Heise area (Morgan and Lageson, 1999; Lageson et al., 1999). The movement of limestone slide blocks in the Palisades Reservoir area between 6.3 and 5.5 Ma indicates that significant topographic relief was present in the Snake Range by at least 5.5 Ma.

Timing of Uplift of the Teton Range, Wyoming

The Teton Range of northwestern Wyoming is one of the most spectacular mountain ranges in the western United States. Previous estimates for the uplift of the Teton Range have placed the maximum age of uplift at 9 to 10 Ma. Love (1977) based this estimate on the results of a single K-Ar date and a fission-track date from two locations in the Miocene Teewinot Formation. Love (1977) also cited the absence of coarse detritus in the Teewinot Formation, now exposed at the base of the Teton Range, as evidence that the Teton Range was not present during Teewinot deposition.

Roberts and Burbank (1993) suggested that the uplift history of the Teton Range was a complex process. They divided the Teton Range into three sections and noted the differential uplift of the central block was ~2 km greater than uplift of the southern and northern blocks. They further noted that the fission-track age distribution along the range front suggested asymmetric cooling and uplift. They proposed that the northern Mount Moran section had a different cooling history and was uplifted later than the central and southern blocks.

The areal distribution of the 4.45 ± 0.05-Ma Kilgore Tuff in Jackson Hole and the Gros Ventre Range suggests that the northern Teton Range could not have been a significant topographic feature at this time. The Kilgore Tuff extends as a densely welded ignimbrite from the eastern SRP to east of the Teton Range and as isolated exposures in the foothills of the Gros Ventre Range (Love et al., 1992; Fig. 2A). Significant topography on the northern Teton Range at 4.5 Ma would have restricted eastward movement of the pyroclastic flow, preventing the emplacement of welded Kilgore Tuff in areas such as Signal Mountain (Figs. 1 and 2A, locality 6) and Pilgrim Peak in Jackson Hole. Pierce and Morgan (1992) suggested that the present episode of hanging wall rotation into the Teton fault of beds exposed east of the fault started after 6 Ma. We suggest here that the episode must have started after 4.5 Ma.

SUMMARY

Field studies and high-precision $^{40}Ar/^{39}Ar$ dates for regional ignimbrites establish a time-stratigraphic framework for the Heise volcanic field in the eastern SRP (Tables 1 and 3, Figs. 4, 5, 6, and 8). The $^{40}Ar/^{39}Ar$ dates resolve preexisting stratigraphic uncertainties and bracket the timing of tectonic events in the region. Our results suggest that four, rather than three (Morgan, 1992), large-volume, Yellowstone-type ignimbrites were erupted from the Heise volcanic field and form the major framework rhyolites of the Heise Group. The $^{40}Ar/^{39}Ar$ dates reported in this study refine the ages of these regional ignimbrites (Fig. 4A) and corroborate previously established correlations, particularly long-distance correlations between exposures on the northern and southern margins of the eastern SRP.

The first caldera-forming event in the Heise volcanic field erupted the greater than 1500 km^3 Blacktail Creek Tuff at 6.62 ± 0.03 Ma. The second large-volume regional ignimbrite erupted from the Heise volcanic field is the 6.27 ± 0.04-Ma Walcott Tuff. $^{40}Ar/^{39}Ar$ dates and other evidence firmly establish the correlation of the Walcott Tuff with the tuff of Blue Creek exposed on the northern margin of the eastern SRP. The volume of the Walcott Tuff is estimated to be less than that calculated for the Blacktail Creek Tuff (Morgan, 1992). A third, smaller, regional ignimbrite, the Conant Creek Tuff, was erupted at 5.51 ± 0.13 Ma; its current distribution is confined to the northern Big Hole and Snake River Ranges near Heise and to the northwestern Teton Range. $^{40}Ar/^{39}Ar$ dates firmly establish the correlation between the type section of the Conant Creek Tuff and the previously named tuff of Elkhorn Spring in the Heise area. The volume of the Conant Creek Tuff is substantially less than that of the Blacktail Creek Tuff. The final large-volume caldera-forming eruption in the Heise volcanic field produced the greater than 1800 km^3 Kilgore Tuff at 4.45 ± 0.05 Ma. The Kilgore Tuff is distributed extensively on both margins of the eastern SRP and extends as far east as Jackson Hole, Wyoming.

The voluminous ash fallouts derived from regional ignimbrite eruptions in the Heise volcanic field were deposited in late Miocene-early Pliocene lakes in basins near present-day Palisades Reservoir. Similar $^{40}Ar/^{39}Ar$ dates and sanidine geochemistry facilitate one-to-one correlations between these distal ash-fall units and regional Heise Group ignimbrites. Ash in lacustrine sediments resting above a 6.8 Ma andesite (Oriel and Moore, 1985) on the northeastern shore of Palisades Reservoir is correlated as fallout from the eruption of the 6.62 ± 0.03-Ma Blacktail Creek Tuff. Other ash units from lacustrine sediments exposed below and near a large detachment block in this area are dated at 6.18 ± 0.22 Ma and 6.35 ± 0.15 Ma and may represent fallout ash from the top of a fractionated magma chamber that erupted the 6.27 ± 0.04-Ma Walcott Tuff. A 7-m-thick plinian-fall deposit overlying the same detachment block dated at 5.56 ± 0.08 Ma and 5.43 ± 0.13 Ma is correlative with the 5.51 ± 0.13-Ma Conant Creek Tuff.

The locations of the calderas in the Heise volcanic field can be determined from a better understanding of the age and distribution characteristics of smaller-volume ignimbrites and rhyolitic lava flows, in combination with characteristics of the regional ignimbrites. Mapping the distribution of rhyolitic lava flows and local ignimbrites and determining their ages better defines evidence for the location of individual vent sources. Evidence for the location of a vent source for the 6.62 ± 0.03-Ma Blacktail Creek Tuff found in the northern Caribou Range on the southern margin of the eastern SRP includes volcanic facies, grain size data from the ignimbrite, and the distribution of rhyolitic lava flows of similar age in the same area. The rhyolite of Milo Dry Farm and the 6.3 ± 0.3-Ma rhyolite of Ching Creek in the Big Hole Mountains may represent eruptions along a ring-fracture zone of the Blacktail Creek caldera. Likewise, evidence for the location of source vents for the Blue Creek caldera, which erupted the 6.27 ± 0.04-Ma Walcott Tuff, exists along the northern margin of the eastern SRP. Evidence for the location of a ring-fracture zone for the Blue Creek caldera along the northern margin of the plain is found in the southern Beaverhead Mountains where the 6.20 ± 0.05-Ma rhyolite of Lidy Hot Springs is present. Its age is statistically indistinguishable from that of the Walcott Tuff. The thickest known section of the Conant Creek Tuff is exposed in the Heise cliffs, overlying the 5.59 ± 0.05-Ma tuff of Wolverine Spring, and near the rhyolite of Kelly Canyon of essentially the same age, 5.7 ± 0.1-Ma (Figs. 4 and 8). The close temporal and spatial relationship between these three units suggests that the tuff of Wolverine Creek and rhyolite of Kelly Canyon are precursors to the eruption of the Conant Creek Tuff. We find three probable source areas for the 4.45 ± 0.05-Ma Kilgore Tuff. Each area is associated with a rhyolitic lava flow of similar age. Juniper Buttes, located in the middle of the eastern SRP and the site of several younger rhyolitic lava flows, is most likely a resurgent dome associated with the Kilgore caldera (Morgan, 1988).

Our $^{40}Ar/^{39}Ar$ age determinations refine the timing of tectonic events associated with detachment faulting in the Snake Range and uplift of the Teton Range. Movement of a fault block containing Mississippian strata in the Snake Range near Palisades Reservoir occurred between 6.3 Ma and 5.51 Ma based on sanidine $^{40}Ar/^{39}Ar$ dates obtained from ash units bounding the slide block. From the characteristics seen in the base of the detachment block and a thick capping plinian-fall deposit, we suggest detachment was sudden and catastrophic. It may have been seismically triggered by the eruption of large volumes of ignimbrite and fall deposits associated with the Conant Creek Tuff. $^{40}Ar/^{39}Ar$ dates from pumice and ash in the thick section of a plinian-fall deposit resting directly above the detachment block and the Conant Creek Tuff are statistically identical. Additionally, the chemistry and mineralogy of the plinian deposit and the Conant Creek Tuff are similar. These data suggest the entire thickness of the plinian-fall deposit represents a discrete volcanic event associated with the eruption of the 5.51 ± 0.13-Ma Conant Creek Tuff.

We are able to put temporal constraints on the uplift of the northern Teton Range from the distribution of the densely welded Kilgore Tuff in Jackson Hole, Wyoming, fingerprinted using paleomagnetic remanence directions (Morgan, 1992), $^{40}Ar/^{39}Ar$ dates, and trace-element chemistry. Based on the age of the Kilgore Tuff at Signal Mountain (Figs. 1 and 2A, locality 6), the northern Teton Range was not a significant topographic feature until after 4.5 Ma.

ACKNOWLEDGMENTS

The authors are indebted to J. David Love for introducing them to the geology of Jackson Hole and vicinity. We would like to acknowledge Timothy Morzel and H.Z. Albedo for assistance in field work, Lisa Peters and Richard Esser for assistance in the New Mexico Geochronology Research Laboratory, Glenn Embree for assistance in measuring some of the stratigraphic sections, Dave Moore and Dave Lageson for discussions regarding the Palisades Reservoir section, Greg Lee and Pat Shanks for help in our index figure and base maps, and Jan, Nathaniel, and Jesse Morzel for field support. We would also like to acknowledge the K/Ar dates provided by G.B. Dalrymple and D.J. Doherty, the $\delta^{18}O$ analyses of quartz crystals provided by W.E. Hildreth, and trace element chemistry for the Conant Creek Tuff provided by R.L. Christiansen. The manuscript was improved greatly with reviews and comments by Steve Harlan, Andrei Sarne-Wojcicki, John Geissman, Pat Shanks, Charles Chapin, Matt Heizler, Roger Stewart, Richard Smith, and Mike McCurry. John Sutter is acknowledged for his enthusiastic encouragement and early support of our work. Special acknowledgments go to Bob Christiansen, David Doherty, J. David Love, Ken Pierce, Betty Skipp, and Bill Hackett for the hours of fruitful discussions over many years regarding the geology of this region.

REFERENCES CITED

Allmendinger, R.W., 1982, Sequence of late Cenozoic deformation in the Blackfoot Mountains, southeastern Idaho, *in* Bonnichsen, B., and Breckenridge, R.M., eds., Cenozoic Geology of Idaho: Idaho Bureau of Mines and Geology Bulletin 26, p. 505–516.

Anders, M.H., 1990, Late Cenozoic evolution of Grand and Swan Valleys, Idaho (field trip no. 1, part 2), *in* Roberts, S., ed., Geologic Field Tours of Western Wyoming and parts of adjacent Idaho, Montana, and Utah:

Geological Survey of Wyoming Public Information Circular 29, p. 15–25.

Anders, M.H., Geissman, J.W., Piety, L.A., and Sullivan, J.T., 1989, Parabolic distribution of circumeastern Snake River Plain seismicity and latest Quaternary faulting: Migratory pattern and association with the Yellowstone hotspot: Journal of Geophysical Research, v. 94, p. 1589–1621.

Anders, M.H., Saltzman, J., and Hackett, W.R., 1997, Borehole WO-2, the Rosetta stone (core) of the Heise volcanics of east central Idaho: Implications for the track of the Yellowstone hotspot: Geological Society of America Abstracts with Programs, v. 29, no. 6, p. A-365.

Armstrong, R.L., Leeman, W.P., and Malde, H.E., 1975, K-Ar dating, Quaternary and Neogene rocks of the Snake River Plain, Idaho: American Journal of Science, v. 275, p. 225–251.

Armstrong, R.L., Harakal, J.E., and Neill, W.M., 1980, K-Ar dating of Snake River Plain (Idaho) volcanic rocks—New results: Isochron/West, no. 27, p. 5–10.

Boyer, S.E., and Hossack, J.R., 1992, Structural features and emplacement of surficial gravity-slide sheets, northern Idaho-Wyoming thrust belt, *in* Link, P.K., Kuntz, M.A., and Platt, L.B., eds., Regional Geology of Eastern Idaho and Western Wyoming: Geological Society of America Memoir 179, p. 197–213.

Byers, F.M., Jr., Carr, W.J., Orkild, P.P., Quinlivan, W.D., and Sargent, K.A., 1976, Volcanic suites and related cauldrons of Timber Mountain-Oasis Valley Caldera Complex, southern Nevada: U.S. Geological Survey Professional Paper 919, p. 70.

Camp, V.E., 1995, Mid-Miocene propagation of the Yellowstone mantle plume head beneath the Columbia River Basalt source region: Geology, v. 23, p. 435–438.

Cande, S.C., and Kent, D.V., 1995, Revised calibration of the geomagnetic polarity time scale for the Late Cretaceous and Cenozoic: Journal of Geophysical Research, v. 100, p. 6093–6095, doi: 10.1029/94JB03098.

Carr, W.J., and Trimble, D.E., 1963, Geology of the American Falls quadrangle, Idaho: U.S. Geological Survey Bulletin 1121-G, 44 p.

Christiansen, R.L., 1984, Yellowstone's magmatic evolution: Its bearing on understanding large volume explosivity, *in* Boyd, F.R., ed., Explosive Volcanism: Inception, Evolution, and Hazards: Washington, D.C., National Academy Press, National Research Council, Studies in Geophysics, p. 84–95.

Christiansen, R.L., 2001, The Quaternary and Pliocene Yellowstone Plateau Volcanic Field of Wyoming, Idaho, and Montana: U.S. Geological Survey Professional Paper 729-G, 145 p.

Christiansen, R.L., and Blank, H.R., 1969, Volcanic evolution of the Yellowstone rhyolite plateau and eastern Snake River Plain, U.S.A. (abs.), *in* Symposium on volcanoes and their roots: Oxford, England, International Association of Volcanology and Chemistry of the Earth's Interior, Volume of Abstracts, p. 220–221.

Christiansen, R.L., and Love, J.D., 1978, The Pliocene Conant Creek Tuff in the northern part of the Teton Range and Jackson Hole, Wyoming: U.S. Geological Survey Bulletin, v. 1435-C, p. 9.

Christiansen, R.L., Foulger, G.R., and Evans, J.R., 2002, Upper-mantle origin of the Yellowstone hotspot: Geological Society of America Bulletin, v. 114, p. 1245–1256, doi: 10.1130/0016-7606(2002)1142.0.CO;2.

Deino, A., and Potts, R., 1990, Single-crystal ^{40}Ar/^{39}Ar dating of the Olorgesailie Formation, southern Kenya Rift: Journal of Geophysical Research, v. 95, p. 8453–8470.

Deino, A., and Potts, R., 1992, Age-probability spectra for examination of singe-crystal ^{40}Ar/^{39}Ar dating results: Examples from Olorgesailie, southern Kenya Rift: Quaternary International, v. 13-14, p. 47–53.

Doherty, D.J., 1976, Ground surge deposits in eastern Idaho [M.S. thesis]: Detroit, Michigan, Wayne State University, 121 p.

Doherty, D.J., 1979, Drilling data from exploration well 2–2A, NW, sec. 15, T. 5 N., R. 31 E., Idaho National Engineering Laboratory, Butte County, Idaho: U.S. Geological Survey Open-file Report, v. 79–851, p. 1.

Embree, G.F., Lovell, M.D., and Doherty, D.J., 1978, Drilling data from the Sugar City geothermal exploration well, Madison County, Idaho: U.S. Geological Survey Open-file Report, v. 78–1095, p. 1.

Fisher, R.V., and Schmincke, H.-U., 1984, Pyroclastic Rocks: Berlin, Springer-Verlag, 472 p.

Humphreys, E.D., Dueker, K.G., Schutt, D.L., and Smith, R.B., 2000, Beneath Yellowstone; evaluating plume and nonplume models using teleseismic images of the upper mantle: GSA Today, v. 10, no. 12, p. 1–7.

Izett, G.A., 1981, Volcanic ash beds: Recorders of upper Cenozoic silicic pyroclastic volcanism in the western United States: Journal of Geophysical Research, v. 86, p. 10,200–10,222.

Janecke, S.U., and Evans, J.C., 1999, Folded and faulted Salt Lake Formation above the Miocene to Pliocene New Canyon and Clifton detachment faults, Malad and Bannock ranges, Idaho: Field trip guide to the Deep Creek Half graben and environs, *in* Hughes, S.S., and Thackray, G.D., eds., Guidebook to the Geology of Eastern Idaho, Idaho Museum of Natural History, p. 71–96.

Kellogg, K.S., and Embree, G.F., 1985, Geologic map of the Stevens Peak and Buckskin Basin areas, Bingham and Bannock counties, Idaho: U.S. Geological Survey Miscellaneous Field Studies Map MF-1854, scale 1:24,000.

Kellogg, K.S., and Marvin, R.F., 1988, New potassium-argon ages, geochemistry, and tectonic setting of upper Cenozoic rocks near Blackfoot, Idaho: U.S. Geological Survey Bulletin 1806, 19 p.

Kellogg, K.S., Harlan, S.S., Mehnert, H.H., Snee, L.W., Pierce, K.L., Hackett, W.R., and Rogers, D.W., 1994, Major 10.2 Ma rhyolitic volcanism in the eastern Snake River Plain, Idaho—Isotopic age and stratigraphic setting of the Arbon Valley Tuff member of the Starlight Formation: U.S. Geological Survey Bulletin, v. 2091, p. 18.

Kuntz, M.A., 1979, Geologic map of the Juniper Buttes area, eastern Snake River Plain, Idaho: U.S. Geological Survey Miscellaneous Investigations Map I-1115, scale 1:24,000.

Kuntz, M.A., Covington, H.R., and Schorr, L.J., 1992, An overview of basaltic volcanism of the eastern Snake River Plain, *in* Link, P.K., Kuntz, M.A., and Platt, L.B., eds., Regional Geology of Eastern Wyoming and Western Wyoming: Geological Society of America Memoir 179, p. 227–267.

Lageson, D.R., Adams, D.C., Morgan, L.A., Pierce, K.L., and Smith, R.B., 1999, Neogene-Quaternary Tectonics and Volcanism of southern Jackson Hole, Wyoming and southeastern Idaho, *in* Hughes, S.S., Thackray, G.D., eds., Guidebook to the Geology of Eastern Idaho: Pocatello, Idaho Museum of Natural History, p. 115–130.

Leeman, W.P., 1982, Rhyolites of the Snake River Plain-Yellowstone Plateau Province, Idaho and Wyoming: A summary of petrogenic models, *in* Bonnichsen, B. and Breckenridge, R.M., eds., Cenozoic Geology of Idaho: Idaho Bureau of Mines and Geology Bulletin 26, p. 193–202.

Love, J.D., 1977, Summary of upper Cretaceous and Cenozoic stratigraphy, and of tectonic and glacial events in Jackson Hole, northwest Wyoming: Wyoming Geological Association Guidebook, 29th Annual Field Conference, p. 585–593.

Love, J.D., Reed, J.C., Jr., and Christiansen, A.C., 1992, Geologic map of Grand Teton National Park, Wyoming: U.S. Geological Survey Miscellaneous Investigations Series Map I-2031, scale 1:62,500.

Love, T.C., 1986, Geochemical correlation of Salt Lake-equivalent pyroclastic deposits in Idaho and Wyoming [M.S. thesis]: New Orleans, University of New Orleans, 114 p.

Malde, H.E., 1991, Quaternary geology and structural history of the Snake River Plain, Idaho and Oregon: Quaternary nonglacial geology: Conterminous U.S., The Geology of North America, v. K-2, p. 251–281.

Manley, C.R., and McIntosh, W.C., 2004, The Juniper Mountain Volcanic Center, Owyhee County, Southwestern Idaho: Age relations and physical volcanology *in* Bonnichsen, B., White, C.M., and McCurry, M., eds., Tectonic and Magmatic Evolution of the Snake River Plain Volcanic Province: Idaho Geological Survey Bulletin 30, p. 205–227.

Mansfield, G.R., and Ross, C.S., 1935, Welded rhyolitic tuffs in southeastern Idaho: Washington, D.C., American Geophysical Union Transactions, 16th Annual Meeting, p. 308–321.

Marvin, R.F., Mehnert, H.H., and Noble, D.C., 1970, Use of ^{26}Ar to evaluate the incorporation of air by ash flows: Geological Society of America Bulletin, v. 81, p. 3385–3392.

McBroome, L.A., 1981, Stratigraphy and origin of Neogene ash-flow tuffs on the north-central margin of the eastern Snake River Plain, Idaho [M.S. thesis]: University of Colorado, 74 p.

McBroome, L.A., Doherty, D.J., and Embree, G.F., 1981, Correlation of major Pliocene and Miocene rhyolites, eastern Snake River Plain, Idaho: Geological Society of Montana Guidebook, Southwest Montana Field Conference, p. 323–330.

McCalpin, J.P., Piety, L.A., and Anders, M.H., 1990, Latest Quaternary faulting and structural evolution of Star Valley, Wyoming (field trip no. 1, part 1), *in* Roberts, S., ed., Geologic Field Tours of Western Wyoming and Parts of Adjacent Idaho, Montana, and Utah: Geological Survey of Wyoming Public Information Circular 29, p. 5–12.

McIntosh, W.C., and Chamberlin, R.M., 1994, ^{40}Ar/^{39}Ar geochronology of Middle to Late Cenozoic ignimbrites, mafic lavas, and volcaniclastic rocks in the Quemado Region, New Mexico: New Mexico Geological Society Guidebook, v. 45, p. 165–185.

McIntosh, W.C., Sutter, J.F., Chapin, C.E., and Kedzie, L.L., 1990, High-precision ^{40}Ar/^{39}Ar sanidine geochronology of ignimbrites in the Mogollon-Datil volcanic field, southwestern New Mexico: Bulletin of Volcanology, v. 52, p. 584–601.

Moore, D.W., Oriel, S.S., and Mabey, D.R., 1987, A Neogene(?) gravity-slide block and associated slide phenomena in Swan Valley graben, Wyoming and Idaho: Geological Society of America Centennial Field Guide, Rocky Mountain Section, v. 1987, p. 113–116.

Morgan, L.A., 1988, Explosive rhyolitic volcanism on the eastern Snake River Plain [Ph.D. dissert.]: Manoa, University of Hawaii, 191 p.

Morgan, L.A., 1992, Stratigraphic relations and paleomagnetic and geochemical correlations of ignimbrites of the Heise volcanic field, eastern Snake River Plain, Idaho and western Wyoming, *in* Link, P.K., Kuntz, M.A., and Platt, L.B., eds., Regional Geology of Eastern Idaho and Western Wyoming: Geological Society of America Memoir 179, p. 215–226.

Morgan, L.A., and Bonnichsen, B., 1989, Heise Volcanic Field, *in* Chapin, C.E., and Zidek, J., eds., IAVCEI (International Association of Volcanology and Chemistry of the Earth's Interior) Field Trip Guide to Silicic Volcanism in the Yellowstone—Snake River Plain Province (Bonnichsen, B., Christiansen, R.L., Morgan, L.A., Moye, F.J., Hackett, W.R., Leeman, W.P., Honjo, N., Jenks, M.D., and Godchaux, M.M.), New Mexico Bureau of Mines & Mineral Resources Memoir 47, p. 153–160.

Morgan, L.A., and Lageson, D.R., 1999, Seismically triggered rapid emplacement of slide blocks in Grand Valley, Idaho, during large-volume ignimbrite eruptions from the Heise volcanic field: Geological Society of America Abstracts with Programs, v. 31, no. 4, p. A50.

Morgan, L.A., Doherty, D.J., and Leeman, W.P., 1984, Ignimbrites of the eastern Snake River Plain, Idaho: Evidence for major caldera-forming eruptions: Journal of Geophysical Research, v. 89, p. 8665–8678.

Morgan, L.A., Pierce, K.L., and McIntosh, W.C., 1997, Inferences for changes in plume dynamics from stratigraphic framework studies of ignimbrites, central Snake River Plain, Idaho: Geological Society of America Abstracts with Programs, v. 29, no. 6, p. A299.

Morgan, W.J., 1972, Plate motions and deep-mantle convection: Geological Society of America Memoir, v. 132, p. 7–22.

Naeser, C.W., Izett, G.A., and Obradovich, J.D., 1980, Fission track and K-Ar ages of natural glasses: U.S. Geological Survey Bulletin, v. 1489, p. 31.

Nielsen, D.L., and Hulen, J.B., 1984, Internal geology and evolution of the Redondo Dome, Valles caldera, New Mexico: Journal of Geophysical Research, v. 89, p. 8695–8712.

North American Commission on Stratigraphic Nomenclature, 1983, North American Stratigraphic Code: American Association of Petroleum Geologists Bulletin, v. 67, no. 5, p. 841–875.

Obradovich, J.D., 1992, Geochronology of the late Cenozoic volcanism of Yellowstone National Park and adjoining areas: Wyoming and Idaho: U.S. Geological Survey Open file Report 92–408, 45 p.

Oriel, S.S., and Moore, D.W., 1985, Geologic map of the West and East Palisades RARE II further planning areas, Idaho and Wyoming: U.S. Geological Survey Miscellaneous Field Studies Map MF-1619-B, scale 1:50,000.

Pederson, J., 1999, A long-term record of climate-controlled hillslope sedimentation [Ph.D. dissertation]: University of New Mexico, 195 p.

Perkins, M.E., and Nash, B.P., 2002, Explosive silicic volcanism of the Yellowstone Hotspot: the ash fall tuff record: Geological Society of America Bulletin, v. 114, no. 3, p. 367–381.

Perkins, M.E., Diffendal, R.F., Jr., and Voorhies, M.R., 1995, Tephrochronology of the Ash Hollow Formation (Ogallala Group)—Northern Great Plains: Geological Society of America Abstracts with Programs, v. 27, no. 3, p. 79.

Perkins, M.E., Brown, F.H., Nash, W.P., McIntosh, W.C., and Williams, S.K., 1998, Sequence, age and source of silicic fallout tuffs in middle to late Miocene basins of the northern Basin and Range Province: Geological Society of America Bulletin, v. 110, no. 3, p. 344–360, doi: 10.1130/0016-7606(1998)1102.3.CO;2.

Pierce, K.L., and Morgan, L.A., 1992, The track of the Yellowstone hot spot: Volcanism, faulting and uplift, *in* Link, P.K., Kuntz, M.A., and Platt, L.B., eds., Regional Geology of Eastern Idaho and Western Wyoming: Geological Society of America Memoir 179, p. 1–53.

Pierce, K.L., Morgan, L.A., and Saltus, R.W., 2004, Yellowstone plume head: Postulated relations to the Vancouver slab, continental boundaries, and climate, *in* Bonnichsen, B., White, C.M., and McCurry, Michael, eds., Tectonic and Magmatic Evolution of the Snake River Plain Volcanic Province: Idaho Geological Survey Bulletin 30, p. 5–33.

Prostka, H.J., and Embree, G.F., 1978, Geology and geothermal resources of the Rexburg area, eastern Idaho: U.S. Geological Survey Open-File Report 78-1009, 15 p., 2 plates.

Rampino, M.R., 1991, Volcanism, climate change, and the geologic record: Society of Economic Paleontologists and Mineralogists Special Publication 45, p. 9–18.

Richards, M.A., Duncan, R.A., and Courtillot, V.E., 1989, Flood basalts and hot spot tracks: Plume heads and tails: Science, v. 246, p. 103–107.

Roberts, S.V., and Burbank, D.W., 1993, Uplift and thermal history of the Teton Range (northwestern Wyoming) defined by apatite fission-track dating: Earth and Planetary Science Letters, v. 118, p. 295–309, doi: 10.1016/0012-821X(93)90174-8.

Rytuba, J.J., and McKee, E.H., 1984, Peralkaline ash flow tuffs and calderas of the McDermitt volcanic field, southeast Oregon and north central Nevada: Journal of Geophysical Research, v. 89, p. 8616–8628.

Samson, S.D., and Alexander, E.C., Jr, 1987, Calibration of the interlaboratory ^{40}Ar-^{39}Ar dating standard, MMhb-1: Chemical Geology, v. 66, p. 27–34.

Sarna-Wojcicki, A.M., Morrison, S.D., Meyer, C.E., and Hillhouse, J.W., 1987, Correlation of upper Cenozoic tephra layers between sediments of the Western United States and eastern Pacific Ocean and comparison with biostratigraphic and magnetostratigraphic age data: Geological Society of America Bulletin, v. 98, p. 207–223.

Scholten, R., Keenmon, K.A., and Kupsch, W.O., 1955, Geology of the Lima region, southwestern Montana, and adjacent Idaho: Geological Society of America Bulletin, v. 66, p. 345–404.

Skipp, B.A., Prostka, H.J., and Schleicher, D.L., 1979, Preliminary geologic map of the Edie Ranch quadrangle, Clark County, Idaho and Beaverhead County, Montana: U.S. Geological Survey Open-File Report 79-845, scale 1:62,500.

Skipp, B.A., Kuntz, M.A., and Morgan, L.A., 1989, Geologic map of the Mackay 4 (Grouse) SE quadrangle, Butte County, Idaho: U.S. Geological Survey Open-File Report 89-431, scale 1:24,000.

Smith, R.B., and Braile, L.W., 1994, The Yellowstone hotspot: Journal of Volcanology and Geothermal Research, v. 61, p. 121–187, doi: 10.1016/0377-0273(94)90002-7.

Smith, R.L., 1960, Zones and zonal variations in welded ash-flow tuffs: U.S. Geological Survey Professional Paper, v. 354F, p. 148–159.

Smith, R.L., and Bailey, R.A., 1968, Resurgent cauldrons: Geological Society of America, v. 116, p. 613–662.

Sparks, R.S.J., and Walker, G.P.L., 1977, The ground-surge deposit: A third type of pyroclastic rock: Nature, v. 241, p. 62–64.

Sparks, R.S.J., Self, S., and Walker, G.P.L., 1973, Products of ignimbrite eruptions: Geology, v. 1, p. 115–118.

Staatz, M.H., and Albee, H.F., 1966, Geology of the Garns Mountain quadrangle, Bonneville, Madison, and Teton counties, Idaho: U.S. Geological Survey Bulletin, v. 1205, p. 122.

Stearns, H.T., and Isotoff, A., 1956, Stratigraphic sequence in the Eagle Rock volcanic area near American Falls, Idaho: Geological Society of America Bulletin, v. 67, p. 19–34.

Steiger, R.H., and Jäeger, E., 1977, Subcommission on geochronology: Convention on the use of decay constants in geo- and cosmochronology: Earth and Planetary Science Letter, v. 36, p. 359–362.

Thompson, G.R., Fields, R.W., and Alt, D., 1982, Land-based evidence for Tertiary climatic variations: Northern Rockies: Geology, v. 10, p. 413–417.

Trimble, D.E., and Carr, W.J., 1976, Geology of the Rockland and Arbon quadrangles, Power County, Idaho: U.S. Geological Survey Geologic Quadrangle Map GQ-1553, scale 1:24,000.

U.S. Geological Survey, 1972, Geologic map of Yellowstone National Park: U.S. Geological Survey Miscellaneous Geologic Investigations Map I-711, scale 1:125,000.

Walker, G.P.L., Self, S., and Froggatt, F.C., 1981, The ground layer of the Taupo ignimbrite: A striking example of sedimentation from a pyroclastic flow: Journal of Volcanology and Geothermal Research, v. 10, p. 1–11, doi: 10.1016/0377-0273(81)90051-2.

Manuscript Received by the Society 7 November 2003
Revised Manuscript Received 29 april 2004
Manuscript Accepted 10 June 2004

Printed in the USA